Refining the biogeographical scenario of the land snail Cornu aspersum aspersum: Natural spatial expansion and human-mediated dispersal in the Mediterranean basin

Stéphanie Sherpa, Armelle Ansart, Luc Madec, Marie-Claire Martin, S. Dréano, Annie Guiller

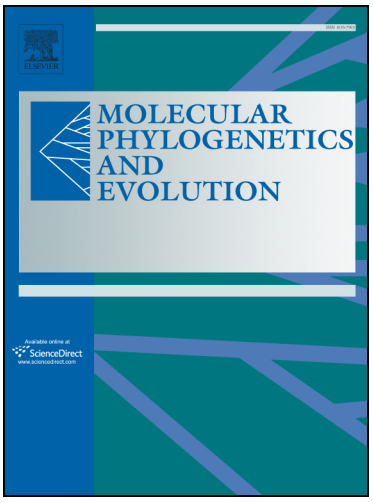

Refining the biogeographical scenario of the land snail *Cornu aspersum aspersum*: natural spatial expansion and human-mediated dispersal in the Mediterranean basin

Stéphanie Sherpa, Armelle Ansart, Luc Madec, Marie-Claire Martin, Stéphane Dréano, Annie Guiller

PII: S1055-7903(17)30900-4
DOI: https://doi.org/10.1016/j.ympev.2017.12.018
Reference: YMPEV 6005

To appear in: *Molecular Phylogenetics and Evolution*

Received Date: 28 April 2016
Revised Date: 24 April 2017
Accepted Date: 12 December 2017

Please cite this article as: Sherpa, S., Ansart, A., Madec, L., Martin, M-C., Dréano, S., Guiller, A., Refining the biogeographical scenario of the land snail *Cornu aspersum aspersum*: natural spatial expansion and human-mediated dispersal in the Mediterranean basin, *Molecular Phylogenetics and Evolution* (2017), doi: https://doi.org/10.1016/j.ympev.2017.12.018

Refining the biogeographical scenario of the land snail *Cornu aspersum aspersum*: natural spatial expansion and human-mediated dispersal in the Mediterranean basin

Stéphanie Sherpa[1]*, Armelle Ansart[1], Luc Madec[1], Marie-Claire Martin[1], Stéphane Dréano[2], Annie Guiller[3]

Affiliation:

[1] Unité de recherche Écosystèmes, Biodiversité, Évolution, CNRS UMR 6553, Université de Rennes 1, Campus de Beaulieu, 35042 Rennes, France

[2] Institut de Génétique & Développement de Rennes, CNRS UMR 629, Université de Rennes 1, Faculté de Médecine, 35043 Rennes, France

[3] Unité de recherche Écologie et Dynamique des Systèmes Anthropisés, CNRS FRE 3498, Université de Picardie Jules Verne, 80000 Amiens, France

*Corresponding Author:

E-mail: stephanie.sherpa@hotmail.fr

Abstract

The land snail *Cornu aspersum aspersum*, native to the Mediterranean region, has been the subject of several anatomical and molecular studies leading to recognize two divergent lineages, named “East” and “West” according to their geographical distribution in North Africa. The first biogeographical scenario proposed the role of Oligocene paleogeographic events and Quaternary glacial refugia to explain spatial patterns of genetic variation. The aim of this study was to refine this scenario using molecular and morphometric data from 169 populations sampled across Mediterranean islands and continents. The two previously described lineages no longer correspond to distinct biogeographical entities. Phylogenetic relationships reveal the existence of seven clades, do not support the Tyrrhenian vicariance hypothesis, and suggest that *C. a. aspersum* most likely originates from North Africa. We found two contrasted patterns with the seven clades defining spatially well-structured populations in the southern Mediterranean whereas one clade is distributed across the basin. High genetic diversities and rates of endemism in North Africa support the role of this region for the diversification of *C. a. aspersum*. In referring to divergence times previously estimated, we suggest allopatric differentiation due to geological changes of the Atlas system and multiple refugial areas during Pleistocene glaciations. The new biogeographical scenario implies an initial range expansion from North Africa to the Iberian Peninsula and the peri-Tyrrhenian regions through land bridges connections during the Messinian Salinity Crisis and Pleistocene glaciations. Historical events appear to have also structured morphometric variation but recent dispersal events favored the emergence of secondary contacts between clades. Southern Mediterranean clades are limited to their initial distribution and populations of the recent clade would have rapidly recolonized the whole Mediterranean in the Holocene due to greater adaptive potential and the influence of human transportations.

Keywords: phylogeography; geometric morphometrics; vicariance; secondary contacts; Gastropoda; Stylommatophora

1. Introduction

Understanding the role of historical and geological changes in generating current patterns of biodiversity is essential to identify processes of divergence and speciation (Moritz et al., 2000; Hewitt, 2004). Phylogeographical studies have significantly improved our knowledge about historical factors influencing species distribution and population divergence through repeated cycles of population contraction/extinction, isolation in refugia, establishment of biogeographic barriers and founder events (Avise and Walker, 1998; Taberlet et al., 1998; Schneider and Moritz, 1999; Moritz et al., 2000; Hewitt, 2000, 2004). The Mediterranean basin provides an outstanding laboratory for such phylogeographical studies because it represents one of the world's major biodiversity hotspots (Médail and Myers, 2004; Thompson, 2005) and a remarkable geographic crossroads for the European, Saharian and Irano-Turanian regions (Quézel, 1985). The inherent species richness of this area helps to elucidate the role of historical vicariance and dispersal in shaping the patterns of present-day species distribution. In this region, biogeographical, palynological and phylogenetic data indicate that the separation and drift of the Betic arch until late Pliocene (2 Myr) (Gueguen et al., 1998; De Jong, 1998; Gelabert et al., 2002), marine transgressions during the Tertiary (5.96–5.33 Myr, Steininger and Rögl, 1984), and Quaternary climatic oscillations (deMenocal, 2004) have affected current spatial patterns of several species complexes (Steinfartz et al., 2000; Fromhage et al., 2004; Veith et al., 2004; Cosson et al., 2005; Pinho et al., 2007; Jakob et al., 2007; Magri et al., 2007; Médail and Diadema, 2009; Pfenninger et al., 2010; Naciri et al., 2010; Kornilios et al., 2010).

Among species widely distributed across the Mediterranean basin, the land snail *Cornu aspersum aspersum* (Müller, 1774) has proved to be a suitable model to understand phylogeographical patterns across North Africa and surrounding regions of the Western basin, and to evaluate hypotheses leading to population differentiation. Studies based on molecular

markers have described two divergent lineages, named “East” and “West” according to their geographical location in North Africa (Guiller et al., 1994, 2001, 2006). Although the exact geographical origin of the subspecies still remains unresolved, the first phylogeographical scenario, based on mitochondrial DNA variation of European and North African populations, assumes that ancestral populations of the subspecies *C. a. aspersum* would have dispersed in the western Mediterranean through microplate tectonics from Oligocene (Guiller and Madec, 2010). Subsequent to the geological development of the Tell Atlas mountain chain, the separation of several continental formations acted as a barrier to gene flow in Algeria, resulting in the differentiation of two lineages. The “East” lineage would have declined due to recurrent climatic fluctuations and glaciation periods from mid-Pliocene to the last Ice Age whereas the “West” lineage would have widely spread to European territories. Although the Tyrrhenian vicariance hypothesis would support the current distribution pattern of other land snail species as *Tudorella* sp (Pfenninger et al., 2010), this scenario is not clearly consistent with migration models tested in *C. a. aspersum* since they showed the species most likely spread from North Africa to Europe (Guiller and Madec, 2010). Furthermore, the geographical distribution of “East” and “West” populations show discontinuities (Guiller and Madec, 2010), which make difficult to understand the biogeographical meaning of these two lineages. The comparison of geographical patterns obtained from different markers should help to evaluate the effect of historical events (Long and Singh, 1995; Magniez-Jannin et al., 2000; Drotz, 2003) and to resolve some uncertainties regarding tree topology. The analysis of anatomical (Madec et al. 1994) and morphological (Madec et al. 2003) traits showed the existence of a geographical splitting in North Africa corresponding to expectations from molecular markers. However, the congruence between molecular and morphometric markers has never been tested.

This work aims refining the previous scenario on the basis of a greatly enriched sampling in both continental and island Mediterranean areas. We analyzed simultaneously neutral molecular (mitochondrial DNA and microsatellite loci) and morphometric (distal genitalia and shell) markers and combined phylogeographic and population genetics methods, traditional morphometrics and landmark-based geometric morphometrics. First, we ask whether the "East" *vs.* "West" terminology is still relevant considering the geographical distribution of these lineages. Especially, we sampled populations in both eastern (Greek islands) and western (Morocco) Mediterranean. Second, we address the relative role played by vicariance events linked to the geological formation of the Mediterranean basin in shaping distribution patterns of the subspecies, disposing of new samples originating from the putative Oligocene microplates (Rif, Calabria, Majorca, Corsica). Third, from the most likely scenario inferred, we evaluate in what extent the historical factors have also structured morphometric variation.

2. Material and Methods

2.1. Sampling and data collection

Samples of *Cornu aspersum aspersum* were collected between 1989 and 2015 in ten different countries (Fig. 1, Table A.1). Out of 169 localities investigated in the present study, 114 localities have already been considered in previous analyses (Madec et al., 1994; Guiller et al., 1994, 2000, 2001, 2012; Guiller and Madec, 2010) whilst 55 new ones of more recently collected specimens were specifically analyzed for the purpose of this work (Corsica, Malta, Morocco, continental South Italy, Majorca, Sicily, Crete, Naxos, continental France). We used two molecular markers (mitochondrial DNA: 16S ribosomal RNA (16S) and cytochrome b (cyt b) genes; microsatellite loci: Ha2, Ha6, Ha8, Ha10 and Ha11) and two morphometric markers (shell size and shape; genital measurements). For mitochondrial data, we compiled

the sequences published in Guiller et al. (2001, Genbank accessions AF126111 to AF126144), in Guiller and Madec (2010, Genbank accessions JX399889 to JX400440), in Guiller et al. (2012, Genbank accessions EU912610 to EU912830) and newly sequenced specimens (Genbank accessions KU996449 to KU997005). Out of 601 16S sequences and 592 cyt b sequences, we newly added 293 and 264 sequences respectively. Both sequences were obtained for 499 individuals. The subspecies *C. a. maximum* was used as outgroup in the phylogenetic analysis. For microsatellite loci, we used the genotypes of 2063 individuals covering 74 populations of which 424 individuals were previously analyzed in Guiller et al. (2012). Shells of 895 adult specimens (53 populations) were used for the geometric morphometrics analysis. In order to provide an overview of the shell variation, pictures of selected specimens are shown in Fig. 3. The genital measurements dataset was composed of 2078 adult specimens (138 populations), of which 972 had already been analyzed in Madec and Guiller (1994). We tried to maximize the number of specimens characterized by both molecular and morphometric markers but given the population-based approach of previous studies, there were many discrepancies between the four datasets. Individuals used in morphometric studies (shells and genitalia measurements; Madec and Guiller 1994, Madec et al. 2003) were not exactly the same as those used for molecular variation (Guiller et al. (2001). Otherwise, geometric morphometrics was not a key issue at that time and shells of specimens from most of the populations were not annotated or preserved. For each population, datasets sample sizes are given in Table A.1. Over all specimens sequenced for mtDNA genes (16S and cyt b), we had a molecular set of 460 individuals genotyped at microsatellite loci, and morphological sets of 264 and 281 specimen shells and genital measurements respectively.

2.2. DNA Extraction, Amplification and Sequençing

Total genomic DNA was obtained from foot and mantle muscles of fresh or alcohol-preserved material using the chelex extraction protocol (Guiller et al., 2001). For mitochondrial genes, we amplified fragments of approximately 360 and 560 bp for the 16S and cyt b respectively (see Thomaz et al., 1996; Guiller and Madec, 2010 for details). For microsatellite genotypes, locus amplification and allele identification were performed as reported in Guiller et al. (2000) with slight modifications. Primer sequences, characteristics and PCR conditions are described in Table A.2.

2.3. Mitochondrial Data Analysis

Mitochondrial sequences were aligned using the CODONCODE ALIGNER software v3.5 (CodonCode Corporation, Dedham, Massachusetts). Analyses of sequence polymorphism were carried out using DnaSP v4.10.9 (Rozas et al., 2003). To infer phylogenetic relationships among individuals, we performed the Bayesian-based inference (BI) implemented in MRBAYES v3.1.1 (Ronquist and Huelsenbeck, 2003). The best-fit model of nucleotide substitutions was selected before using the Akaike Information Criterion with MrAIC v1.4.2 (Nylander et al., 2004). For both genes, the best model was GTR, with symmetrical substitution matrix, unequal base frequencies, a parameter for invariable sites (I) and a gamma distribution parameter that describes rate variation across variable sites (Γ). We analyzed genes simultaneously in concatenated 16S and cyt b sequences into an alignment of 926 bp. The posterior probabilities of trees and parameters were approximated with Markov Chain Monte Carlo (MCMC) and Metropolis coupling. Each chain was run for 10,000,000 cycles (2 runs each four chains) with trees sampled every 100 generations. Posterior probabilities were obtained from the 50% majority rule consensus of trees sampled after discarding the trees saved before chains reached apparent stationarity (after several thousand

generations). The average standard deviation of split frequencies after 10,000,000 generations was 0.00718, indicating a good convergence between the two runs.

2.4. Microsatellite Loci Analysis

Genotypes of 2063 individuals were used to detect population genetic structure and explore the relationships between island and continental populations. We performed a Discriminant Analysis of Principal Components (DAPC, Jombart et al., 2010) with the number of populations as clusters, using the Adegenet R package v1.4.2 (Jombart, 2008). We also used Bayesian algorithms implemented in STRUCTURE v2.3.3 (Pritchard et al., 2000) to assign individuals to K virtual populations without priors on geographical locations. The model used assumes recent ancestry of individuals (admixture) and current gene flow (correlated allele frequencies) between populations. For each value of K, we carried out 10 independent Markov Chain Monte Carlo (MCMC) runs with 5,000 iterations discarded as burn-in followed by an additional 50,000 generations. The *ad hoc* statistic ΔK suggested by Evano et al. (2005) was used to determine the optimal number of clusters.

2.5. Morphometric Analyses

Geometric morphometrics – Shells were digitalized in apertural view using numeric images (Reflex Canon E07D camera) after transformation in tps format using TpsUtil v1.38 (Rohlf, 2006). Landmarks (LM) and semilandmarks (SLM) were used to describe shell shape (Fig. 2). Digitalization was achieved with TpsDig2 v2.12 (Rohlf, 2008). Eight LM, of which two were of type I (LM1, LM4), two of type II (LM5, LM6) and others of type III (Bookstein, 1991, 1997; Slice et al., 1996) have been combined with two curves manually traced of 50 and 20 equidistant SLM anchored on LM6-7 and LM7-8 respectively. Variation due to scale, orientation and position was removed using Procrustes superimposition in CoordGen8

(Sheets, 2008). Procrustes coordinates have then been aligned with SemiLand6 using the minimum Procrustes distance (Sheets et al., 2004). We performed the Principal Component Analysis (PCA) implemented in PCAGen8 (Sheets, 2008).

Distal genitalia – Fully developed genitalia were obtained from living organisms or preserved in 70% ethanol. Each one was scored for genital measurements (Fig. 3) as described in Madec and Guiller (1994): length of penis and following part of epiphallus from genital atrium up to the penial retractor (PL); length of proximal part of epiphallus (EL); length of flagellum (FL); length of *vas deferens* (VDL); lengths of proximal (BL1) and distal (BL2) part of bursa copulatrix duct; length of bursa copulatrix diverticulum (DL); length of dart sac (DSL). Variation in genital measurements was summarized using a double centering PCA on log-transformed lengths with the ade4 R package v1.6-2 (Chessel et al., 2004). An instrumental variable was also added to remove potential storing effects explaining 2% of the total variance.

2.6. Molecular and morphometric congruence

We used each of the three sets of individuals characterized by microsatellite genotypes, shell traits, and genital measurements (460, 264 and 281 individuals respectively). Nine composite variables from multivariate analyses were used based on individual scores on the retained principal components (PCs from morphometric analyses) or linear discriminants (LDs from DAPC). In order to evaluate the congruency of morphometric variation with mtDNA variation, we tested the correlation between morphometric and phylogenetic distances by using Mantel tests (with standard Bonferroni correction) implemented in the vegan R package v2.2-1 (Oksanen et al., 2013). Pairwise phylogenetic distances were obtained using branch length in the two genes consensus tree (BI analysis) and pairwise individual-based distances for each morphometric variable were calculated using individual scores. We also tested the

correlation between phylogenetic distances and pairwise genetic distances (DSA, Shared Allele Distances) calculated using microsatellite genotypes according to the Bowcock et al. (1994) method implemented in the prabclus R package v2.2-6 (Hennig and Hausdorf, 2006). Differences in mtDNA clade means for each of the nine composite variables were investigated using one-way analyses of variance (ANOVAs) and multiple comparison tests (with standard Bonferroni correction). All the statistical analyses were performed with the R software v3.3.1 (R Developmental Core Team).

3. Results

3.1. Phylogenetic relationships

The BI phylogram calculated with concatenated alignments (16S and cyt b) showed well-resolved topology with high support values (Fig. 3). Phylogenetic relationships among 499 individuals revealed seven clades:

- Clade A corresponds to Moroccan sequences, which comprises seven individuals from populations M7 and M9.
- Clade B corresponds to sequences from western Algerian populations (A1 and A2), Italy and Spain. This clade splits into two highly supported sub-groups. The first one comprises sequences from both A1 and A2 populations and four sequences from I16. The second clustered two individuals from A1 with individuals from Galicia (E9 and E13).
- Clade C comprises 155 sequences divided into two subgroups. The first subgroup corresponds to sequences from four populations in Algeria (A14 to A17). The most basal node of the second subgroup was weakly supported, resulting in a wide haplogroup with sequences originating from many geographical locations: Algeria (A18 to A24), Corsica (Co2, Co4, Co9, Co10), Sicily (Si2 to Si6), Malta (Ma3 to Ma6), southern Italy (I9 to I14, I16, I17) and Tunisia (T2, T3).

- Clade D corresponds to individuals from three populations in Tunisia (T1, T4, T6).
- Clade E clusters populations from Morocco (M5 and M6) with some specimens from I12 (Italy).
- Clade F is underrepresented, with only two individuals from Kabylia (A13.7 and A13.8).
- Clade G is the widest, with 286 individuals. It comprises individuals from Algeria (A3 to A13), Morocco (M4, M10), France (F39 to F41, F48 to F52), Spain (E2, E9, E13, E14, E16), Italy (I15, I16), Majorca (Ba2 to Ba8), Crete (Ct1 to Ct9), Naxos (Nx1 to Nx3), Malta (Ma5), Corsica (Co2, Co5, Co9), and Sicily (Si1, Si2).

Among the 169 populations considered, eight from Galicia in Spain (E9 and E13), Corsica (Co2, Co9), Italy (I12 and I16), Malta (Ma5) and Sicily (Si2) were scattered in different clades, defining mixed populations. The current spatial distribution of haplogroups revealed that clades C and G have large geographical distribution in the Mediterranean basin (Fig. 1). The geographical structure in North Africa showed the co-occurrence of the seven clades, which define distinct spatial entities. Three clades (A, D, F) were endemic to North Africa and most of within-clade subgroups show Algerian specimens branches off from the basal nodes.

3.2. Mitochondrial variability

Sequences of the 16S (369 bp) obtained for 601 individuals covered a number of 170 mutations and 111 polymorphic sites. The 557 bp sequences of the cyt b region analyzed for 592 individuals revealed a total of 432 mutations and 272 polymorphic sites. Both genes showed high nucleotide diversity (0.045 ± 0.001 for 16S and 0.102 ± 0.001 for cyt b) and high haplotype diversity (0.979 ± 0.002 for 16S and 0.994 ± 0.001 for cyt b), covering 177 haplotypes of which 111 were unique for 16S and 291 haplotypes of which 197 were unique

for cyt b (excluding sites with gaps and missing data). Haplotype diversity results were similar for the two genes but nucleotide diversity was greater for cyt b (Table 1).

Genetic diversity was also estimated according to mtDNA (BI analysis) and geographical subdivisions (Table 1). Haplotype diversity ranged from 0.530 ± 0.136 to 0.974 ± 0.039 for 16S and from 0.848 ± 0.104 to 0.982 ± 0.004 for cyt b. The lowest haplotype diversity was recorded for clade E. Each haplogroup showed high nucleotide diversity, except clade A. Clades E, F and G showed the highest nucleotide diversities despite a small number of sequences analyzed in clades E and F. Haplotype and nucleotide diversities were also high according to geographical subdivisions. Mainland samples originating from France and Croatia showed the lowest nucleotide diversity whilst Algerian, Italian, Moroccan and Spanish sequences showed the highest. Regarding islands, the nucleotide diversity was low in populations from Majorca, Crete and Naxos and high in those from Corsica and Sicily.

3.3. Population structuring

Variation at five microsatellite loci exhibited a low level of spatial structuring. In the DAPC, scatterplot of LD1 *vs.* LD2 did not show clear separation with respect to geographical subdivisions (Fig. 4a). Only populations from Naxos showed genotypic differentiation on LD1. The discrimination between populations also revealed high allelic variation within Italian, Corsican, Sicilian, Moroccan, and Naxos populations. In the Bayesian STRUCTURE analysis, the optimal number of genetic clusters in the successive K-means procedure was three (K=3) but many populations showed strong admixture, precluding their assignment to one genetic cluster. For K=3, one genetic cluster comprises all Algerian populations, E9, E13 and E14 from Spain, I15 from Italy and, M4, M5 and M10 in Morocco. The second cluster showed genetic similarities between Corsican, Italian (except I15), Maltese (except Ma5) and Sicily. The third genetic cluster gathered all populations from Majorca and Crete, and some

populations from France (except F49, F50), Morocco (M7, M8, M9) and Tunisia (T6). The two first described genetic clusters formed a unique one at K=2. Levels of sub-structure between K=4 to K=7 allowed to identify groups of populations corresponding to their geographical location. We found genetic similarities among populations from Crete at K=4, populations from Malta at K=5, populations from Naxos at K=6, and populations from Sicily at K=7.

Genotypic variation among the 460 individuals used to test the congruence with mtDNA variation is represented in Fig. 4b. We detected differences in mean genotypes between clades on LD1 and LD2 (ANOVAs, $p<0.001$), and phylogenetic distances were correlated to DSA (Mantel, $r=0.15$, $p<0.001$) (Table 2). Scatterplot on LD1 *vs.* LD2 did not show overlap between clade D and clades B, C and F (Fig. 4b). The average genotype of individuals in clade D was different from those of clades C and G on LD1 (Fig. 8a). Clades C and G had the biggest variation in allelic frequencies, probably due to the large number of within-clade individuals and originating from various geographically isolated locations. Nonetheless, individuals within clade C were differentiated from all clades but F (Fig. 8a). Genotypic differentiation was mainly explained by five alleles on LD1 (Ha2.298, Ha2.300, Ha6.156, Ha8.166, Ha10.223) and five alleles on LD2 (Ha2.290, Ha2.300, Ha2.346, Ha6.156, Ha10. 217) (Fig. 4c).

3.4. Morphometric variation

Based on the results of PCA on shell Procrustes coordinates, the three first principal components, which account for 66% of the total variance, were retained to represent shell morphology (Fig. 6). PC1 (28.5%) was interpreted as shell shape with high scores indicating elongated shells opposed to more globular ones (Fig. 6c). PC2 (21.5%) was interpreted as a variation in aperture size, high scores indicating shells with large aperture (Fig. 6d). PC3

(16.1%) was interpreted as aperture shape with high scores for shell with oval aperture opposed to rounded aperture for low scores (Fig. 6e). Scatterplots of PC1 *vs.* PC2 showed great variation of specimens within main geographical subdivisions (Fig. 6a). Average shape (centroids per population) on these two PCs revealed that some Corsican and Maltese populations (Co4, Co10, Co2, Ma3, Ma4) have elongated shells with a large aperture; populations A18, M7 and T2 have elongated shells with a small aperture; populations F48 and F49 have globular shells with a small aperture and; Naxos populations have globular shells with a large aperture (Fig. 6a). Variations in aperture shape (PC3) and shell size among main geographical subdivisions are given in Figs. A.1 and A.2 respectively.

The three first principal components of the PCA based on genital measurements explained 61% of total variance (Fig. 7). High scores on PC1 (29.1%) were obtained for individuals with long diverticulum and flagellum and a short BL2. PC2 (16.7%) opposed individuals according to the lengths of their BL1 and epiphallus. PC3 (15.1%) showed differentiation based on the size of *vas deferens*, love dart and BL1 (Fig. A.3). Average scores (centroids per population) on scatterplots of PC1 *vs.* PC2 showed that French populations (F39, F51 and F13) had the longest flagellum and diverticulum whereas Algerian A17 and A18 had the smallest. A17 and A18 also had the longest proximal part of the bursa copulatrix duct (BL1) and the smallest epiphallus, contrary to Sardinian (Sa1) and French (F15, F20) populations (Fig 7a). Variation among main geographical subdivisions on PC3 is given in Fig. A.3.

3.5 Congruence between morphometric and mitochondrial variation

We detected significant differences in shell traits and genital measurements that were related to mtDNA variation (Table 2). Average shell shape (PC1), aperture size (PC2), aperture shape (PC3) and shell size (Log Centroid Size) showed significant differences between mtDNA clades (ANOVAs) but only morphometric distances based on shell shape showed strong

correlation with phylogenetic distances (Mantel, r=0.19, p<0.001). Although significant, correlations between phylogenetic distances and distances based on aperture size and the log centroid size were very low. Concerning genital measurements, analysis of variance revealed differences in mean DL, FL and BL2 (PC1) and mean VDL, DSL and BL1 (PC3) between clades but only morphometric distances based on DL, FL and BL2 were significantly correlated to phylogenetic distances (Mantel, r=0.12, p<0.001) (Table 2).

Mean shell shapes in clades A, B, C and D were not significantly different from each other but different from those in clades F and G (Fig 8b). Clades A, B, C, D have elongated shells (high average scores on PC1) and clades F and G have globular shells (low average scores on PC1) (Figs. 6b and 8b). Regarding aperture size (PC2), clades A, B and D had significantly lower average scores (small aperture) than clade C (large aperture) and clades E, F and G were not significantly different from A, B, C and D (Figs. 6b, 6d and 8b). The only difference detected concerns clade B, showing lower average scores (rounded aperture) than clades C, E, G (oval aperture) (Figs. 6b, 6c and 8b). Concerning shell size, clades C and E had small shells, clade G had shells of intermediate size and clades A, B and D had large shells (Fig 8b).

It was not possible to include individuals representing clades D and F for genital measurements. Clades E, C and G had significantly different lengths of diverticulum, flagellum and distal part of the bursa copulatrix duct (PC1, Fig 8c), respectively small, intermediate and long diverticulum and flagellum (Fig 7b). Concerning *vas deferens* and love dart lengths (PC3), clade D showed lower average scores than clades C, E and G (Fig 8c).

4. Discussion

4.1 Geographical origin of C. a. aspersum

The land snail *Cornu aspersum* is native to Mediterranean countries and comprises a set of endemic forms and subspecies in North Africa (Taylor, 1913). The most common subspecies

C. a. aspersum, which is widely distributed in the Mediterranean region, could originate in North Africa according to historical reports (Taylor, 1913) or in Europe in referring to the Tyrrhenian vicariance hypothesis (Guiller and Madec, 2010).

Genetic analyses of taxa distributed on both sides of the Mediterranean Sea mostly support a North African origin, but geological changes related to the tectonic evolution in the western Mediterranean are causal for current distribution patterns of many species (Husemann et al., 2013 for a review). During the Oligocene (30-22 Myr), the Tyrrhenian plate located between the Iberian margin and Southern France split in several microplates that are now found in the Rif range (Morocco), the Balearic Islands, the Kabylies (Algeria), Corsica, Sardinia, and Calabria (southern Italy) (Lonergan and White, 1997; Gueguen et al., 1998; Rosenbaum et al., 2002). Amongst several phylogeographical studies dealing with Mediterranean land snail species (Douris et al., 1998; Schilthuizen et al., 2004; Parmakelis et al., 2005; Ketmaier et al., 2006, 2010; Fiorentino et al., 2008, 2013; Jesse et al., 2011; Chueca and Ohiana, 2011; Prévot et al., 2013), meaningful comparisons covering the entire Mediterranean basin either support the Tyrrhenian vicariance hypothesis (Pfenninger et al., 2010) or a North African origin (Greve et al., 2010; Daümer et al., 2012). In the present study, the reconstruction of phylogenetic relationships among individuals suggests a Moroccan origin, which is consistent with historical reports and migration models showing that *C. a. aspersum* most likely spread from North Africa to European territories (Guiller and Madec, 2010). Furthermore, fossil records from late Pliocene to middle Pleistocene do not obviously support a so old origin of the subspecies (Pallary, 1901; Caziot, 1911; Caziot and Maury, 1912; Taylor, 1913; Paul, 1984).

4.2 Diversification in North Africa

The Mediterranean eco-region of North Africa, expected to be the differentiation center of many taxa (Myers et al., 2000), has been argued to be that of *C. a. aspersum* (Guiller and Madec, 2010). The fine-scale description of spatial patterns in North Africa based on molecular (Guiller et al., 1994, 2001) and morphometric (Madec and Guiller, 1994; Madec et al., 2003) markers revealed two divergent groups of populations recognized as distinct lineages (East *vs*. West). The biogeographical history inferred from hundred populations representative of the distribution range in the western Mediterranean and European coastline (Guiller et al., 2006; Guiller and Madec, 2010) used the "East" and "West" terminology despite the lack of biogeographical meaning outside North Africa. Indeed, "West" haplotypes are distributed in the eastern (Crete, Turkey, Greece) and northern (France) Mediterranean, and "East" haplotypes in western (Portugal) and central Mediterranean (Guiller and Madec, 2010). The present phylogenetic analysis does not support monophyletic groups corresponding to previously described lineages and should thus no longer be considered for inferring broad scale colonization scenarios in the Mediterranean. Relationships among 499 individuals show seven well-supported evolutionary clades based on mtDNA variation. The geographical distributions of clades do not overlap in North Africa and we found high genetic diversities and rate of endemism, suggesting that this area constituted a hot spot of richness. This pattern of haplotype differentiation among geographically close populations may be explained by restricted gene flow between groups of populations and long-term presence of this subspecies in the region, again supporting a North African origin.

The differentiation between Moroccan (clade A) and Algerian populations raises two hypotheses: the formation of a geographical barrier (i.e. vicariance) and the colonization of new environments (i.e. dispersal). Two geographical barriers in eastern Morocco can be involved to explain a historical split between Morocco and Algeria. The Moulouya River has already been suggested as a major cause of differentiation (Guiller and Madec, 2010; Nicolas

et al., 2014) but secondary events in the Atlas system, such as the formation of the "Morocco Hot Line" (MHL), may have also represented a strong geographical barrier. Volcanism in the late Quaternary related to the development of the MHL was restricted to the Middle Atlas region in eastern Morocco (Frizon de Lamotte et al., 2008). As all of our samples in Morocco are located on the west of these two putative barriers, we can only suggest that the differentiation between populations in Morocco and Algeria occurred somewhere eastward. Many Pliocene and Pleistocene fossils from North Africa were described, especially in Oran in western Algeria (Pallary, 1901). Unfortunately, it is not possible to attribute the fossilized shells to extant clades. Tectonic evolution in North Africa was not at that time restricted to Morocco but common in the entire Maghreb (Frizon de Lamotte et al., 2008). The Tell Atlas in Algeria may have also contributed to isolate groups of populations in northern Algeria, leading to differentiation of clade C (populations in eastern Algeria) from clade B (populations A1 and A2 in central Algeria).

The diversification of numerous species in the Mediterranean basin involves climatic fluctuations during Pleistocene by repeated cycles of population expansion to low elevations during cold periods and to high elevations during interglacial periods (Jesse et al., 2011; Poretta et al., 2011; Hewitt, 2011; Solà et al., 2013; Salvi et al., 2013; Kindler et al., 2013; Planas et al., 2014). The topographic heterogeneity across major parts of North Africa and the strong spatial structure of haplotypes could support the scenario of multiple refugia for *C. a. aspersum* (Hughes et al., 2004). Differentiation patterns imply at least three putative refugia in Algeria (clades B, C, D) and two in Morocco, suggested by the two sympatric clades A and E in the Rif region. In eastern Algeria, the retreat of populations may have enhanced differentiation of clade D to the East (in Tunisia) and clade G to the West (central Algeria) from clade C (Edough Peninsula near A20). However, it is more challenging to link putative refugium to the geographical origin of clade G since populations are present in both Algeria

and western Morocco. Concerning clade F, which comprises two individuals from A13 in central Kabylia, it probably represents the contact zone between isolated groups of populations of clade C and G and has already been discussed in previous studies (Guiller and Madec, 2010 and references therein).

If the current genetic diversity originated in different geographical areas, secondary contacts with no or limited gene flow could emerge near lineage boundaries. In North Africa, we found evidence that microsatellite genotypes and some morphological traits are also geographically structured. The sympatric clades A and E in Morocco show two distinct genetic clusters in the Bayesian clustering analysis, and shell shape and distal genitalia were divergent. Isolated groups of populations probably became differentiated from each other, having their own evolutionary trajectories, but we cannot suggest that this morphological differentiation is the result of adaptive (selection) or non-adaptive (genetic drift) process. Contradictory results arise from genotypic similarities in seven populations from Algeria representative of three clades found in this region (B, G, C), suggesting high intermixing. Nonetheless, we detected differentiation in some shell traits and lengths of genital organs between these clades. Especially, clades C and G show divergent lengths of producing-spermatophore organs (flagellum, epiphallus) and receiving-spermatophore organs (diverticulum, bursa copulatrix duct). These organs are likely to co-evolve under the influence of sexual selection (Anthès et al., 2008; Sauer and Hausdorf, 2009) and to induce pre-copulatory reproductive isolation (Koene and Schulenburg, 2005). Current dispersal and gene flow thus may be due to insufficient morphological differences compared to those between clade E and clades A and G.

4.3 Natural range expansion

C. a. aspersum is currently distributed in both European and North African continents and western Mediterranean islands. A strong geographical barrier, the Mediterranean Sea, thus separates populations. Two possible ways of colonization, depending on the geologic time scale, could support the current distribution of haplotypes. They refer to the Messinian Salinity Crisis in the late Miocene (MSC, 5.96 to 5.33 Myr; Krijgsman et al., 1999; Duggen et al., 2003) and climatic fluctuations during the Pleistocene (1.65 to 0.01 Myr; deMenocal, 2004). These events both resulted in connections between Europe and North Africa through land bridges between Iberia and Morocco (Strait of Gilbraltar) and between Tunisa, Sicily and Italy (Strait of Sicily).

The decrease in sea level during the MSC facilitated migration on both sides of the western Mediterranean and the refilling of the Mediterranean Sea (5.3 Myr) caused the diversification of many taxa (Fromhage et al., 2004; Martinez-Solano et al., 2004; Stöck et al., 2012). However, the lack of genetic differentiation between eastern Algeria and the peri-Tyrrhenian regions (clade C), and between western Algeria/Morocco, Balearic Islands and Spain (clade G) indicates recent exchanges between islands and continents. Divergence time estimates in Guiller and Madec (2010) suggests that the spread of this subspecies to Europe did probably not occur earlier than late Pleistocene. However, some fossils record outside North Africa indicate that *C. a. aspersum* was already present in late Pliocene in southern France (Caziot et Maury, 1912) and the Balearic Islands (Paul, 1984), suggesting that the subspecies probably started to spread during the MSC. Although fossil records are not available before in the peri-Tyrrhenian regions (Middle Pleistocene in Corsica, Caziot, 1911), only the sea level during the MSC may have allowed large enough connections between Corsica, Sicily, Italy, Malta and Algeria to explain the distribution of clade C. Furthermore, many Italian, Corsican, Maltese and Sicilian show similarities in the Bayesian cluster analysis, supporting their post-Messinian isolation from Algerian populations.

Periodic growth of ice sheets during Pleistocene on land in high latitudes and mountains may have induced population expansion/decline cycles in northern Mediterranean that can explain fossilized shells from this period in southern France (Caziot, 1911). In late Pleistocene and Holocene, glacial advances considerably reduced oversea distances resulting in the possible colonization of Europe and islands in central Mediterranean of species already well differentiated in North Africa (Cosson et al., 2005; Carranza et al., 2006; Santos et al., 2012). Although clade G could have initially spread to Iberia from Morocco (strait of Gibraltar) or from Algeria (Almeria-Oran Front, Patarnello et al., 2007), the major cause for rapid population demographic and spatial expansion is probably the Holocene postglacial climate optimality, as assumed for several land snails species (Pfeninger and Posada, 2002; Pinceel et al., 2005; Dépraz et al., 2008).

Considering that many haplotypes from the European continent and Mediterranean islands are nested within African clades, we support a dispersal center in North Africa. Southern Mediterranean clades are located under the Last Glaciation Margin (LGM), suggesting that populations have been impeded in their dispersal and limited to their initial southern distribution. Postglacial recolonization of Europe and eastern Mediterranean seems only imply the spatial expansion of clade G, suggesting a greater adaptive potential. It worth noting that for clades A, B, C and D restricted to geographical regions under the LGM, specimens possess elongated shells whereas those of clade G have more globular ones.

4.4 Human-mediated dispersal

The influence of human-mediated dispersal in shaping land snails biogeographical patterns has already been mentioned and thus need to be considered carefully (Jesse et al., 2011; Daümer et al., 2012; Fiorentino et al., 2016). The recently diverged clade G is present on diverse and disjointed geographical areas including islands and several identified contact

zones between clades (Galicia, Corsica, Sicily and southern Italy). This pattern does not coincide with those expected as a result of natural processes in organisms with poor dispersal abilities. As many species in the helicid genera, *C. a. aspersum* has been deliberately introduced through the Mediterranean for food delicacy and the spread across the whole Mediterranean probably occurred in the recent past as a consequence of anthropogenic dispersal. Only clade G is present in the eastern Mediterranean and the lack of any fossil record in continental Greece and Greek Islands (Naxos and Crete) indicate that *C. a. aspersum* has been deliberately introduced in this region. Low nucleotide diversities in Naxos, Crete, Balearic Islands and France, and the homogenous genetic background in each of these regions suggest that all individuals share common ancestry, supporting the influence of human activities. There are no direct proof of intentional shipping of snails in the antiquity, but dispersal of *C. a. aspersum* as early as the Bronze Age (3300 BP) has been documented in Greece and Greek islands (Welter-Schultes, 2008) and was probably initiated by the Romans in northwestern Europe (Guiller, 1994). Among the different contact zones identified in the present study, populations are located either near commercial port (Bastia, Co9 and Palermo, Si1, Si2) or big cities (Ajaccio, Co2) in Corsica and Sicily. In the Maltese archipelago, three populations (clade C) are located in Gozo Island while the mixed populations is in Malta. Still highly commercialized, the dispersal of this land snail could be even more recent as stated by collection reports in eastern and northern Europe (e. g. Austria, Czech Republic, Juřičková and Kapounek, 2009).

5. Conclusions

The aim of this study was to revise the previous biogeographical scenario of *C. a. aspersum* by assessing the geographical origin of clades in the Mediterranean and the historical events responsible for the current distribution of haplotypes. Analyses of mitochondrial, multilocus

genotypes (microsatellite) and morphometric profiles indicate a diversification and dispersal center of this subspecies in North Africa and suggest the role of (i) vicariance events related to geological evolution of the Atlas system and refugia during Pleistocene climatic fluctuations, (ii) both the Messinian Salinity Crisis and Pleistocene glaciations in the natural range expansion of populations, (iii) human activities on the recent expansion of one clade in the entire Mediterranean basin.

The morphological differentiation of the most widespread clade suggests differences in adaptive and invasive potential, also supported by analyzing invasive populations outside Europe (Guiller et al., 2012). Population history may have influenced the evolution of different shells between clades but variation in shell traits is generally explained by local environmental conditions (Goodfriend, 1986; Heller, 1987; Chiba and Davison, 2007; Anderson et al., 2007; Okajima and Chiba, 2013; Noshita et al., 2012). An intraspecific comparative approach will allow to quantify the relative contribution of historical *vs.* contemporary (i.e. selection) constraints acting on shell variation in *C. a. aspersum* (Sherpa et al., in preparation).

Data accessibility

Mitochondrial DNA sequences are available at the Genbank sequence database (accession numbers AF126111 to AF126144; JX399889 to JX400440; EU912610 to EU912830 and KU996449 to KU997005).

Reference

Anderson, T.K., Weaver, K.F., Guralnick, R.P., 2007. Variation in adult shell morphology and life-history traits in the land snail *Oreohelix cooperi* in relation to biotic and abiotic factors. J. Mollus. Stud. 73, 129−137.

Anthes, N., Schulenburg, H., Michiels, N.K., 2008. Evolutionary links between reproductive morphology, ecology and mating behavior in opisthobranch gastropods. Evolution 62, 900−916.

Avise, J.C., Walker, D., Johns, G.C., 1998. Speciation durations and Pleistocene effects on vertebrate phylogeography. Proc. R. Soc. Lond., B, Biol. Sci. 265, 1707−1712.

Bookstein, F.L., 1991. Morphometric tools for landmark data: geometry and biology. Cambridge University Press.

Bookstein, F.L., 1997. Landmark methods for forms without landmarks: morphometrics of group differences in outline shape. Med. Image Anal. 1, 225−243.

Bowcock, A.M., Ruiz-Linares, A., Tomfohrde, J., Minch, E., Kidd, J.R., Cavalli-Sforza, L.L., 1994. High resolution of human evolutionary trees with polymorphic microsatellites. Nature 368, 455−457.

Carranza, S., Arnold, E.N., Pleguezuelos, J.M., 2006. Phylogeny, biogeography, and evolution of two Mediterranean snakes, *Malpolon monspessulanus* and *Hemorrhois hippocrepis* (Squamata, Colubridae), using mtDNA sequences. Mol. Phylogenet. Evol. 40, 532–546.

Caziot, E., 1911. Étude révisionnelle des Mollusques quaternaires des brèches de Toga à Bastia (Corse). Bull. Soc. Géol. Fr. 11, 239–248.

Caziot, E., Maury, E., 1912. Faune des Mollusques pléistocènes des limons et alluvions caillouteuses de la vallée inférieure du Var près de son embouchure et quelques autres points du même horizon géologique des Alpes Maritimes. Mem. Soc. Zoo. Fr. 25, 45–62.

Chessel D., Dufour, A.B., Thioulouse, J., 2004. The ade4 package-I-One-table methods. R news 4, 5−10.

Chiba S., Davison A., 2007. Shell shape and habitat use in the North-west Pacific land snail *Mandarina polita* from Hahajima, Ogasawara: current adaptation or ghost of species past? Biol. J. Linn. Soc. 91, 149–159.

Chueca, L.J., Oihana, R., 2011. Phylogeny and phylogeography of the genus *Sphincterochila* (Gastropoda, Pulmonata, Helicoidea). The Malacologist 56, 5.

Cosson, J.F., Hutterer, R., Libois, R., Sara, M., Taberlet, P., Vogel, P., 2005. Phylogeographical footprints of the Strait of Gibraltar and Quaternary climatic fluctuations in the western Mediterranean: a case study with the greater white-toothed shrew, *Crocidura russula* (Mammalia: Soricidae). Mol. Ecol. 14, 1151−1162.

Däumer, C., Greve, C., Hutterer, R., Misof, B., Haase, M., 2012. Phylogeography of an invasive land snail: natural range expansion versus anthropogenic dispersal in *Theba pisana pisana*. Biol. Invasions 14, 1665−1682.

De Jong, H., 1998. In search of historical biogeographic patterns in the western Mediterranean terrestrial fauna. Biol. J. Linn. Soc. 65, 99−164.

DeMenocal, P.B., 2004. African climate change and faunal evolution during the Pliocene–Pleistocene. Earth Planet. Sc. Lett. 220, 3−24.

Dépraz, A., Cordellier, M., Hausser, J., Pfenninger, M., 2008. Postglacial recolonization at a snail's pace (*Trochulus villosus*): confronting competing refugia hypotheses using model selection. Mol. Ecol., *17*, 2449−2462.

Douris, V., Cameron, R.A., Rodakis, G.C., Lecanidou, R., 1998. Mitochondrial Phylogeography of the Land Snail *Albinaria* in Crete: Long-Term Geological and Short-Term Vicariance Effects. Evolution 52, 116−125.

Drotz, M.K., 2003. Speciation and mitochondrial DNA diversification of the diving beetles *Agabus bipustulatus* and *A. wollastoni* (Coleoptera, Dytiscidae) within Macaronesia. Biol. J. Linn. Soc. 79, 653−666.

Duggen, S., Hoernle, K., Van Den Bogaard, P., Rüpke, L., Morgan, J.P., 2003. Deep roots of the Messinian salinity crisis. Nature 422, 602−606.

Evanno, G., Regnaut, S., Goudet, J., 2005. Detecting the number of clusters of individuals using the software STRUCTURE: a simulation study. Mol. Ecol., 14, 2611−2620.

Fiorentino, V., Manganelli, G., Giusti, F., Ketmaier, V., 2016. Recent expansion and relic survival: Phylogeography of the land snail genus *Helix* (Mollusca, Gastropoda) from south to north Europe. Mol. Phylogenet. Evol. 98, 358−372.

Fiorentino, V., Manganelli, G., Giusti, F., Tiedemann, R., Ketmaier, V., 2013. A question of time: the land snail *Murella muralis* (Gastropoda: Pulmonata) reveals constraints on past ecological speciation. Mol. Ecol. 22, 170−186.

Fiorentino, V., Salomone, N., Manganelli, G., Giusti, F., 2008. Phylogeography and morphological variability in land snails: the Sicilian *Marmorana* (Pulmonata, Helicidae). Biol. J. Linn. Soc. 94, 809−823.

Frizon de Lamotte, D., Saint Bezar, B., Bracène, R., Mercier, E., 2000. The two main steps of the Atlas building and geodynamics of the western Mediterranean. Tectonics 19, 740−761.

Fromhage, L., Vences, M., Veith, M., 2004. Testing alternative vicariance scenarios in Western Mediterranean discoglossid frogs. Mol. Phylogenet. Evol. 31, 308−322.

Gelabert, B., Sabat, F., Rodríguez-Perea, A., 2002. A new proposal for the late Cenozoic geodynamic evolution of the western Mediterranean. Terra Nova 14, 93−100.

Goodfriend, G.A., 1986. Variation in land-snail shell form and size and its causes: a review. Syst. Biol. 35, 204−223.

Greve, C., Hutterer, R., Groh, K., Haase, M., Misof, B., 2010. Evolutionary diversification of the genus *Theba* (Gastropoda: Helicidae) in space and time: A land snail conquering islands and continents. Mol. Phylogenet. Evol. 57, 572−584.

Gueguen, E., Doglioni, C., Fernandez, M., 1998. On the post-25 Ma geodynamic evolution of the western Mediterranean. Tectonophysics 298, 259−269.

Guiller, A., 1994. Aspect géographique de la différenciation génétique des populations de l'escargot terrestre *Helix aspersa* Müller (Gastéropode Pulmoné). PhD Thesis, University of Rennes, France.

Guiller, A., Arnaud, J.F., Vautrin, D., Solignac, M., 2000. Highly polymorphic microsatellite markers in the landsnail *Helix aspersa* (Mollusca Gastropoda). Mol. Ecol. 9, 1191−1193.

Guiller, A., Bellido, A., Coutelle, A., Madec, L., 2006. Spatial genetic pattern in the land mollusc *Helix aspersa* inferred from a 'centre-based clustering'procedure. Genet. Res. 88, 27−44.

Guiller, A., Coutellec-Vreto, M.A., Madec, L., Deunff, J., 2001. Evolutionary history of the land snail *Helix aspersa* in the Western Mediterranean: preliminary results inferred from mitochondrial DNA sequences. Mol. Ecol. 10, 81−87.

Guiller, A., Madec, L., 2010. Historical biogeography of the land snail *Cornu aspersum*: a new scenario inferred from haplotype distribution in the Western Mediterranean basin. BMC Evol. Biol. 10, 18.

Guiller, A., Madec, L., Daguzan, J., 1994. Geographical patterns of genetic differentiation in the landsnail *Helix aspersa* Müller (Gastropoda: Pulmonata). J. Mollus. Stud. 60, 205−221.

Guiller, A., Martin, M.C., Hiraux, C., Madec, L., 2012. Tracing the invasion of the Mediterranean land snail *Cornu aspersum aspersum* becoming an agricultural and garden pest in areas recently introduced. PloS One 7, e49674.

Heller J., 1987. Shell shape and land-snail habitat in a Mediterranean and desert fauna. Biol. J. Linn. Soc. 31, 257−272.

Hennig, C., Hausdorf, B., 2006. Design of dissimilarity measures: A new dissimilarity between species distribution areas, in: Batagelj, V., Bock, H.H., Ferligoj, A., Žiberna, A. (Eds.), Data Science and Classification. Springer Berlin Heidelberg, pp. 29−37.

Hewitt, G., 2000. The genetic legacy of the Quaternary ice ages. *Nature* 405, 907−913.

Hewitt, G.M., 2004. Genetic consequences of climatic oscillations in the Quaternary. Philos. Trans. R. Soc. Lond., B, Biol. Sci. 359, 183−195.

Hewitt, G.M., 2011. Quaternary phylogeography: the roots of hybrid zones. Genetica 139, 617–638.

Hirano, T., Kameda, Y., Kimura, K., Chiba, S., 2015. Divergence in the shell morphology of the land snail genus *Aegista* (Pulmonata: Bradybaenidae) under phylogenetic constraints. Biol. J. Linn. Soc. 114, 229–241.

Hughes, P.D., Gibbard, P.L., Woodward, J.C., 2004. Quaternary glaciation in the Atlas Mountains of North Africa. Dev. Quat. Sci. 2, 255−260.

Husemann, M., Schmitt, T., Zachos, F.E., Ulrich, W., Habel, J C., 2013. Palaearctic biogeography revisited: evidence for the existence of a North African refugium for Western Palaearctic biota. J. Biogeogr. *41*, 81–94.

Jakob, S.S., Ihlow, A., Blattner, F.R., 2007. Combined ecological niche modelling and molecular phylogeography revealed the evolutionary history of *Hordeum marinum* (Poaceae)—niche differentiation, loss of genetic diversity, and speciation in Mediterranean Quaternary refugia. Mol. Ecol.16, 1713−1727.

Jesse, R., Véla, E., Pfenninger, M., 2011. Phylogeography of a land snail suggests trans-Mediterranean Neolithic transport. PLoS One 6, e20734.

Jombart, T., 2008. adegenet: a R package for the multivariate analysis of genetic markers. Bioinformatics 24, 1403−1405.

Jombart, T., Devillard, S., Balloux, F., 2010. Discriminant analysis of principal components: a new method for the analysis of genetically structured populations. BMC Genet. 11, 94.

Juřičková, L., Kapounek, F., 2009. *Helix* (*Cornu*) *aspersa* (OF Müller, 1774)(Gastropoda: Helicidae) in the Czech Republic. Malacol. Bohemoslov 8, 53−55.

Ketmaier, V., Giusti, F., Caccone, A., 2006. Molecular phylogeny and historical biogeography of the land snail genus *Solatopupa* (Pulmonata) in the peri-Tyrrhenian area. Mol. Phylogenet. Evol. 39, 439−451.

Ketmaier, V., Manganelli, G., Tiedemann, R., Giusti, F., 2010. Peri-Tyrrhenian phylogeography in the land snail *Solatopupa guidoni* (Pulmonata). *Malacologia* 52, 81−96.

Kindler, C., Böhme, W., Corti, C., Gvoždík, V., Jablonski, D., Jandzik, D., Metallinou, M., Široký, P., Fritz, U., 2013. Mitochondrial phylogeography, contact zones and taxonomy of grass snakes (*Natrix natrix*, *N. megalocephala*). Zool. Scr. 42, 458−472.

Koene, J.M., Schulenburg, H., 2005. Shooting darts: co-evolution and counter-adaptation in hermaphroditic snails. BMC Evol. Biol. 5, 1.

Kornilios, P., Kyriazi, P., Poulakakis, N., Kumlutaş, Y., Ilgaz, Ç., Mylonas, M., Lymberakis, P., 2010. Phylogeography of the ocellated skink *Chalcides ocellatus* (Squamata, Scincidae), with the use of mtDNA sequences: A hitch-hiker's guide to the Mediterranean. Mol. Phylogenet. Evol. 54, 445−456.

Krijgsman, W., Hilgen, F.J., Raffi, I., Sierro, F.J., Wilson, D.S., 1999. Chronology, causes and progression of the Messinian salinity crisis. Nature 400, 652−655.

Lonergan, L., White, N., 1997. Origin of the Betic-Rif mountain belt. Tectonics 16, 504−522.

Long, A.D., Singh, R.S., 1995. Molecules versus morphology: the detection of selection acting on morphological characters along a cline in *Drosophila melanogaster*. Heredity 74, 569−581.

Madec, L., Bellido, A., Guiller, A., 2003. Shell shape of the land snail *Cornu aspersum* in North Africa: unexpected evidence of a phylogeographical splitting. Heredity 91, 224−231.

Madec, L., Guiller, A., 1994. Geographic variation of distal genitalia in the landsnail *Helix aspersa* (Mollusca: Gastropoda). J. Zool. 233, 215−231.

Magniez-Jannin, F., David, B., Dommergues, J.L., Su, Z.H., Okada, T.S., Osawa., 2000. Analysing disparity by applying combined morphological and molecular approaches to French and Japanese carabid beetles. Biol. J. Linn. Soc. 71, 343−358.

Magri, D., Fineschi, S., Bellarosa, R., Buonamici, A., Sebastiani, F., Schirone, B., Simeone, M.C., Vendramin, G.G., 2007. The distribution of *Quercus suber* chloroplast haplotypes matches the palaeogeographical history of the western Mediterranean. Mol. Ecol. 16, 5259−5266.

Martínez-Solano, I., Gonçalves, H.A., Arntzen, J.W., García-París, M., 2004. Phylogenetic relationships and biogeography of midwife toads (Discoglossidae: Alytes). J. Biogeogr. 31, 603−618.

Médail, F., Diadema, K., 2009. Glacial refugia influence plant diversity patterns in the Mediterranean Basin. J. Biogeogr. 36, 1333−1345.

Médail, F., Myers, N., 2004. Mediterranean Basin, in: Mittermeier, R.A., Robles Gil, P., Hoffman, M., Pilgrim, J., Brooks, T., Mittermeier, C.G., Lamoreux, J., Da Fonseca, G.A.B. (Eds.), Hotspots revisited: Earth's biologically richest and most endangered terrestrial ecoregions. CEMEX (Monterrey), Conservation International (Washington) and Agrupación Sierra Madre (Mexico), pp. 144−147.

Moritz, C., Patton, J.L., Schneider, C.J., Smith, T.B., 2000. Diversification of rainforest faunas: an integrated molecular approach. Annu. Rev. Ecol. Evol. Syst. 31, 533−563.

Myers, N., Mittermeier, R.A., Mittermeier, C.G., Da Fonseca, G.A., Kent, J., 2000. Biodiversity hotspots for conservation priorities. Nature 403, 853−858.

Naciri, Y., Cavat, F., Jeanmonod, D., 2010. *Silene patula* (Siphonomorpha, Caryophyllaceae) in North Africa: A test of colonisation routes using chloroplast markers. Mol. Phylogenet. Evol. 54, 922−932.

Nicolas, V., Ndiaye, A., Benazzou, T., Souttou, K., Delapre, A., Denys, C., 2014. Phylogeography of the North African dipodil (Rodentia: Muridae) based on cytochrome-b sequences. J. Mamm. 2, 241−253.

Noshita, K., Asami, T., Ubukata, T., 2012. Functional constraints on coiling geometry and aperture inclination in gastropods. Paleobiology 38, 322−334.

Nylander, J.A.A., Ronquist, F., Huelsenbeck, J.P., Nieves-Aldrey, J.L., 2004. Bayesian phylogenetic analysis of combined data. Syst. Biol. 53, 47−67.

Okajima, R., Chiba, S., 2013. Adaptation from restricted geometries: the shell inclination of terrestrial gastropods. Evolution 67, 429−437.

Oksanen, J., Blanchet, F.G., Kindt, R., Legendre, P., Minchin, P.R., O'Hara, R.B., Simpson, G.L., Solymos, P., Stevens, M.H.H., Wagner, H., 2013. Package 'vegan': Community ecology package.

Pallary, P., 1901. Mémoire sur les Mollusques fossiles terrestres, fluviatiles et saumâtres de l'Algérie. Mem. Soc. Géol. Fr. Paléont. 22.

Parmarkelis, A., Pfenninger, M., Spanos, L., Papagiannakis, G., Louis, C., Mylonas, M., 2005. Inference of a radiation in *Mastus* (Gastropoda, Pulmonata, Enidae) on the island of Crete. Evolution 59, 991−1005.

Patarnello, T., Volckaert, F.A., Castilho, R., 2007. Pillars of Hercules: is the Atlantic–Mediterranean transition a phylogeographical break?. Mol. Ecol. 16, 4426−4444.

Paul, C.R.C., 1984. Pleistocene non-marine molluscs from Cova de Ca Na Reia, Eivissa. Soc. Hist. Nat. Balears 28, 95−114.

Pfenninger, M., Posada, D., 2002. Phylogeographic history of the land snail *Candidula unifasciata* (Helicellinae, Stylommatophora): fragmentation, corridor migration, and secondary contact. Evolution 56, 1776−1788.

Pfenninger, M., Véla, E., Jesse, R., Elejalde, M.A., Liberto, F., Magnin, F., Martínez-Ortí, A., 2010. Temporal speciation pattern in the western Mediterranean genus *Tudorella* P. Fischer, 1885 (Gastropoda, Pomatiidae) supports the Tyrrhenian vicariance hypothesis. Mol. Phylogenet. Evol. 54, 427−436.

Pinceel, J.A.N., Jordaens, K., Pfenninger, M., Backeljau, T., 2005. Rangewide phylogeography of a terrestrial slug in Europe: evidence for Alpine refugia and rapid colonization after the Pleistocene glaciations. Mol. Ecol. 14, 1133−1150.

Pinho, C., Harris, D.J., Ferrand, N., 2007. Contrasting patterns of population subdivision and historical demography in three western Mediterranean lizard species inferred from mitochondrial DNA variation. Mol. Ecol. 16, 1191−1205.

Planas, E., Saupe, E.E., Lima-Ribeiro, M.S., Peterson, A.T., Ribera, C., 2014. Ecological niche and phylogeography elucidate complex biogeographic patterns in *Loxosceles rufescens* (Araneae, Sicariidae) in the Mediterranean Basin. BMC Evol. Biol. 14, 195.

Porretta, D., Canestrelli, D., Urbanelli, S., Bellini, R., Schaffner, F., Petric, D., Nascetti, G., 2011. Southern crossroads of the Western Palaearctic during the Late Pleistocene and their imprints on current patterns of genetic diversity: insights from the mosquito *Aedes caspius*. J. Biogeogr. 38, 20−30.

Prévot, V., Jordaens, K., Sonet, G., Backeljau, T., 2013. Exploring species level taxonomy and species delimitation methods in the facultatively self-fertilizing land snail genus *Rumina* (Gastropoda: Pulmonata). PLoS One 8, e60736.

Pritchard, J.K., Stephens, M., Donnelly, P., 2000. Inference of population structure using multilocus genotype data. Genetics 155, 945−959.

Quézel, P., 1985. Definition of the Mediterranean region and the origin of its flora, in: Gomez-Campo, C. (Ed.), Plant conservation in the Mediterranean area. Geobotany 7, 9−24.

R Core Team, 2013. R: A language and environment for statistical computing. R Foundation for Statistical Computing, Vienna, Austria. URL http://www.R-project.org/.

Rohlf, F.J., 2006. Program TpsUtil, version 1.38. Department of Ecology and Evolution. State University of New York at Stony Brook.

Rohlf, F.J., 2008. Program TpsDig, version 2.12. Department of Ecology and Evolution. State University of New York at Stony Brook.

Ronquist, F., Huelsenbeck, J., 2003. MrBayes 3: Bayesian phylogenetic inference under mixed models. Bioinformatics 19, 1572−1574.

Rosenbaum, G., Lister, G.S., Duboz, C., 2002. Reconstruction of the tectonic evolution of the western Mediterranean since the Oligocene. J. Virt. Exp. 8, 107−130.

Rozas, J., Sánchez-DelBarrio, J.C., Messeguer, X., Rozas, R., 2003. DnaSP, DNA polymorphism analyses by the coalescent and other methods. Bioinformatics 19, 2496−2497.

Salvi, D., Harris, D.J., Kaliontzopoulou, A., Carretero, M.A., Pinho, C., 2013. Persistence across Pleistocene ice ages in Mediterranean and extra-Mediterranean refugia: phylogeographic insights from the common wall lizard. BMC Evol. Biol. 13, 147.

Santos, X., Rato, C., Carranza, S., Carretero, M.A., Pleguezuelos, J.M., 2012. Complex phylogeography in the Southern Smooth Snake (*Coronella girondica*) supported by mtDNA sequences. J. Zool. Syst. Evol. Res. 50, 210−219.

Sauer, J., Hausdorf, B., 2009. Sexual selection is involved in speciation in a land snail radiation on Crete. Evolution 63, 2535−2546.

Schilthuizen, M., Gutteling, E., Van Moorsel, C.H.M., Welter-Schultes, F.W., Haase, M., Gittenberger, E., 2004. Phylogeography of the land snail *Albinaria hippolyti* (Pulmonata: Clausiliidae) from Crete, inferred from ITS-1 sequences. Biol. J. Linn. Soc. 83, 317−326.

Schneider, C., Moritz, C., 1999. Rainforest refugia and Australia's Wet Tropics. P. R. Soc. Lond., B, Biol. Sci. 266, 191−196.

Sheets, H.D., 2008. IMP: integrated morphometrics package. Department of Physics, Canisius College, Buffalo, New York.

Slice, D.E., Bookstein, F.L., Marcus, L.F., Rohlf, F.J., 1996. Appendix I: a glossary for geometric morphometrics. NATO ASI Ser., Ser A. 284, 531−552.

Solà, E., Sluys, R., Gritzalis, K., Riutort, M., 2013. Fluvial basin history in the northeastern Mediterranean region underlies dispersal and speciation patterns in the genus *Dugesia* (Platyhelminthes, Tricladida, Dugesiidae). Mol. Phylogenet. Evol. 66, 877−888.

Steinfartz, S., Veith, M., Tautz, D., 2000. Mitochondrial sequence analysis of *Salamandra* taxa suggests old splits of major lineages and postglacial recolonizations of Central Europe from distinct source populations of *Salamandra salamandra*. Mol. Ecol. 9, 397−410.

Steininger, F.F., Rögl, F., 1984. Paleogeography and palinspastic reconstruction of the Neogene of the Mediterranean and Paratethys. Geol. Soc. Lond., SP. 17, 659−668.

Stöck, M., Dufresnes, C., Litvinchuk, S.N., Lymberakis, P., Biollay, S., Berroneau, M., Borzée, A., Ghali, K., Ogielska, M., Perrin, N., 2012. Cryptic diversity among Western Palearctic tree frogs: postglacial range expansion, range limits, and secondary contacts of three European tree frog lineages (*Hyla arborea* group). Mol. Phylogenet. Evol. 65, 1−9.

Susko E., 2014. Bayesian long branch attraction bias and corrections. Syst. Biol. 0, 1−13.

Taberlet, P., Fumagalli, L., Wust-Saucy, A.G., Cosson, J.F., 1998. Comparative phylogeography and postglacial colonization routes in Europe. *Mol. Ecol.* 7, 453−464.

Taylor, J.W., 1913. Monograph of the land and freshwater mollusca of the British Isles. Taylor Brothers, Leeds, pp. 236−273.

Thomaz, D., Guiller, A., Clarke, B., 1996. Extreme divergence of mitochondrial DNA within species of pulmonate land snails. P. R. Soc Lond., B, Biol. Sci. 263, 363−368.

Thompson, J.N., 2005. The geographic mosaic of coevolution. University of Chicago Press.

Veith, M., Mayer, C., Samraoui, B., Barroso, D.D., Bogaerts, S., 2004. From Europe to Africa and vice versa: evidence for multiple intercontinental dispersal in ribbed salamanders (Genus *Pleurodeles*). J. Biogeogr. 31, 159−171.

Welter-Schultes, F.W., 2008. Bronze Age shipwreck snails from Turkey: First direct evidence for oversea carriage of land snails in antiquity. J. Mollus. Stud. 74, 79−87.

Figure captions

Fig. 1. Collection sites of *Cornu aspersum aspersum*. Black dots mark the location of sample sites for which mtDNA was not analyzed. Sample site colors indicate the mitochondrial group of populations inferred from BI analysis (see insert) and the putative distribution range of mtDNA clades is represented.

Fig. 2. (a) Shell geometric morphometrics: black points represent landmarks (LM1 to LM8). LM1 is located at the apex of the shell (Type I landmark: biological homology); LM5 and LM6 are located at the outer extremities of the apertural lip (Type II landmarks: geometrical homology); LM2, LM3, LM8 are located at sutures between whorls, LM4 at the junction of the suture and the lip, and LM7 at the last whorl outer extremity (Type III landmarks: depend of shell position and orientation). Red dotted curves represent the 70 semilandmarks used between LM6 and LM8. (b) Genitalia of *Cornu aspersum aspersum* (gonad and part of sperm oviduct excluded). BC: bursa copulatrix; proximal (BL1) and distal (BL2) parts of the bursa copulatrix duct; D: diverticulum; DS: dart sac; E: epiphallus; F: flagellum; GP: genital pore; MG: digitiform glands; P: penis; PR: penial retractor muscle; S: spermoviduct; V: vagina; VD: *vas deferens*.

Fig. 3. Phylogenetic relationships among *C. a. aspersum* samples inferred with concatenated mitochondrial sequences (16S and cyt b) with *Cornu aspersum maximum = C. a. max.* as outgroup. (a) Schematic representation of BI topology with respective clades. (b) Fifty-percent majority-rule consensus phylogram from BI analysis. Posterior probabilities are indicated at the nodes by black and red dots for high values or by exact values in italics. Sequence labels are abbreviated as in Table A.1. The colors of the clades correspond to those used in Figures 1, 3, 4, 5, 6 and 7. Selected shell specimens covering all clades are shown.

Fig. 4. DAPC on microsatellites genotypes performed with 74 populations as prior clusters. DAPC scatterplot of LD1 *vs.* LD2 is shown for (a) the 2063 individuals analyzed grouped according to main geographical subdivisions, (b) the 460 individuals used to test the congruence with mtDNA variation (BI analysis, Fig. 3). (c) Contributions of alleles on LD1 and LD2.

Fig. 5. Population structure inferred from Bayesian STRUCTURE analyses (admixture, allele frequencies correlated) using five microsatellite loci for different values of K. Each genetic cluster is represented by a color and vertical bards represent individuals. Each vertical bar represents an individual.

Fig. 6. PCA on shell Procrustes coordinates. Scatterplot of PC1 *vs.* PC2 is shown for (a) the 895 individuals analyzed grouped according to main geographical subdivisions, (b) the 264 individuals used to test the congruence with mtDNA variation (BI analysis, Fig. 3). Maximum deformations associated with (c) PC1, (d) PC2 and (e) PC3 are reconstructed from deformation grids and vectors. Only landmarks have been represented and connected for better visualization.

Fig. 7. PCA on genitalia measurements. Scatterplot of PC1 *vs.* PC2 is shown for (a) the 2078 individuals analyzed grouped according to main geographical subdivisions, (b) the 281 individuals used to test the congruence with mtDNA variation (BI analysis, Fig. 3).

Fig. 8. Differences in mtDNA clades means for each of the nine composite variables from

multivariate analyses. Box-plots represent (a) average individuals scores on LD1 and LD2 of the DPAC on microsatellite data, (b) average individuals scores on PC1, PC2 and PC3 of PCA on shell Procrustes coordinates and average log centroid size, (c) average individuals scores on PC1, PC2 and PC3 of the PCA on genitalia measurements. Microsatellite sample size: A=6, B=26, C=137, D=8, E=12, F=2, G=269; shell sample size: A=5, B=22, C=87, D=6, E=8, F=2, G=154; genitalia sample size: A=7, B=4, C=101, E=10, G=159. Letters indicate significant differences between groups (after Bonferroni correction).

Fig. 1

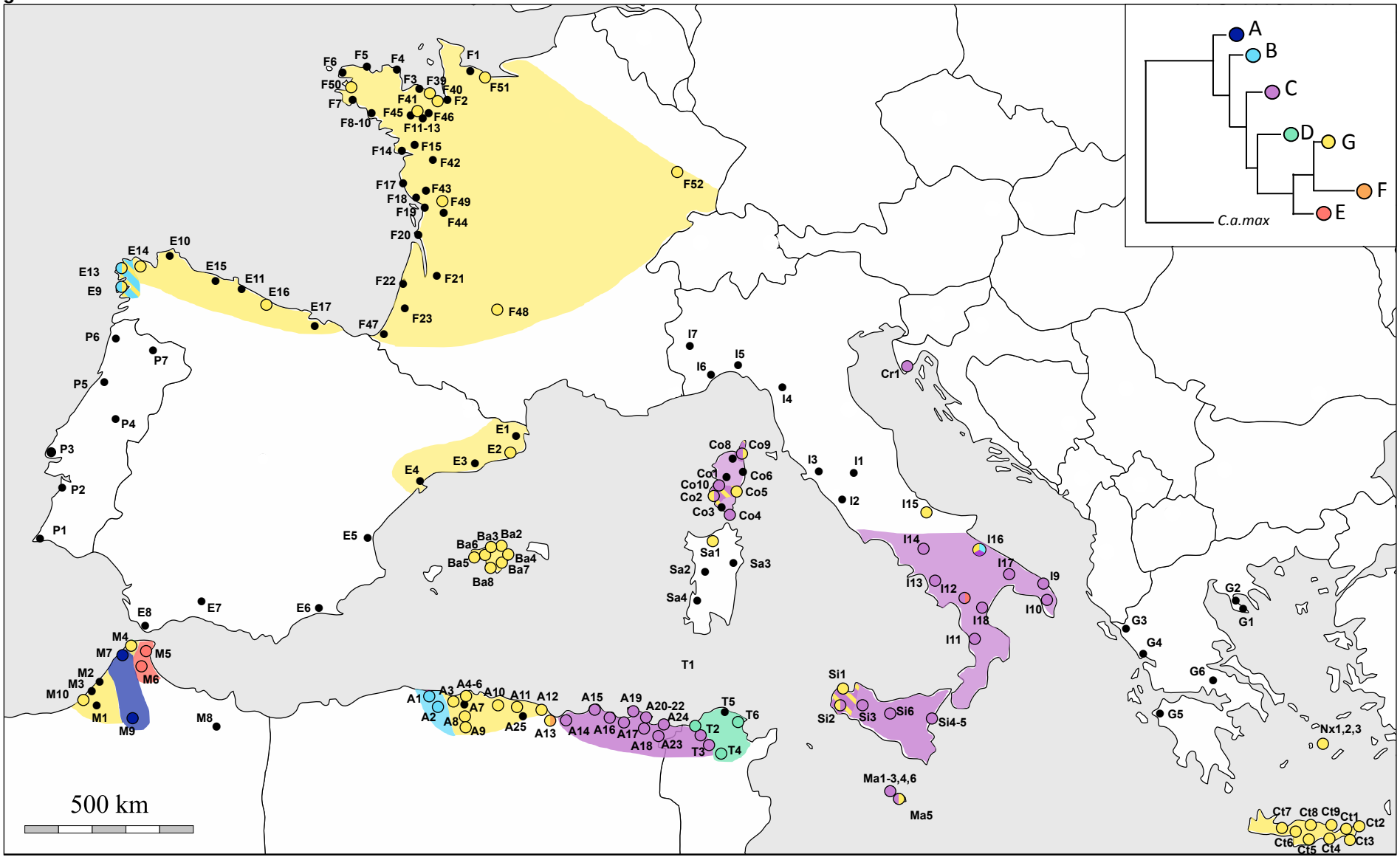
A
B
C
D
G
F
E
C.a.max
F1
F2
F3
F4
F5
F6
F7
F8-10
F11-13
F14
F15
F17
F18
F19
F20
F21
F22
F23
F39
F40
F41
F42
F43
F44
F45
F46
F47
F48
F49
F50
F51
F52
E1
E2
E3
E4
E5
E6
E7
E8
E9
E10
E11
E13
E14
E15
E16
E17
P1
P2
P3
P4
P5
P6
P7
I1
I2
I3
I4
I5
I6
I7
I9
I10
I11
I12
I13
I14
I15
I16
I17
I18
Cr1
Co1
Co2
Co3
Co4
Co5
Co6
Co8
Co9
Co10
Sa1
Sa2
Sa3
Sa4
Ba2
Ba3
Ba4
Ba5
Ba6
Ba7
Ba8
T1
T2
T3
T4
T5
T6
A1
A2
A3
A4-6
A7
A8
A9
A10
A11
A12
A13
A14
A15
A16
A17
A18
A19
A20-22
A23
A24
A25
M1
M2
M3
M4
M5
M6
M7
M8
M9
M10
Si1
Si2
Si3
Si4-5
Si6
Ma1-3,4,6
Ma5
G1
G2
G3
G4
G5
G6
Nx1,2,3
Ct1
Ct2
Ct3
Ct4
Ct5
Ct6
Ct7
Ct8
Ct9
500 km

Fig. 2

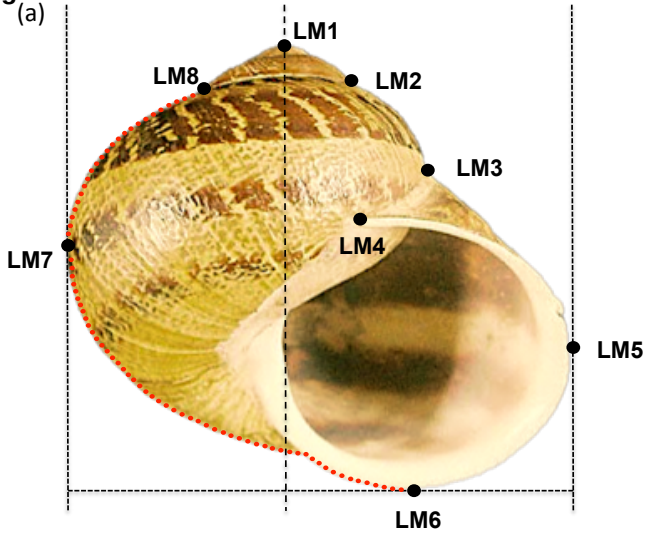
(a)
LM1
LM8
LM2
LM3
LM7
LM4
LM5
LM6

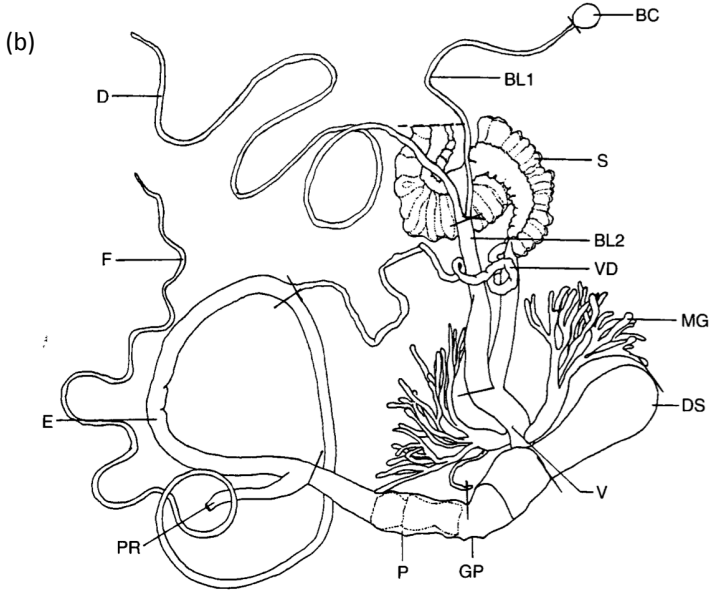
(b)
BC
BL1
D
S
BL2
F
VD
MG
DS
E
V
PR
P
GP

Fig. 3

(b)

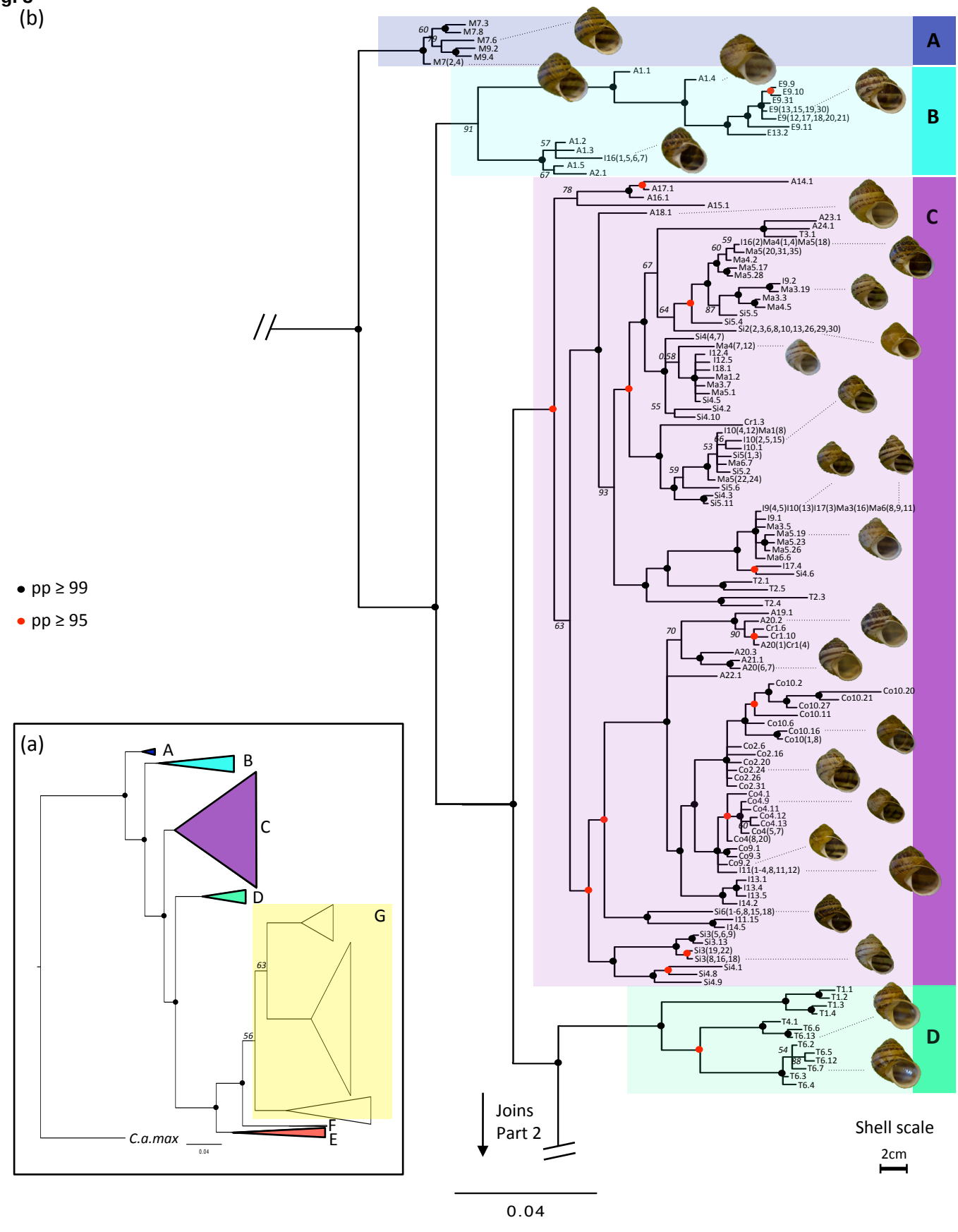
A
B
C
D
M7.3
M7.8
M7.6
M9.2
M9.4
M7(2,4)
A1.1
A1.4
E9.9
E9.10
E9.31
E9(13,15,19,30)
E9(12,17,18,20,21)
E9.11
E13.2
A1.2
A1.3
I16(1,5,6,7)
A1.5
A2.1
A14.1
A17.1
A16.1
A15.1
A18.1
A23.1
A24.1
T3.1
I16(2)Ma4(1,4)Ma5(18)
Ma5(20,31,35)
Ma4.2
Ma5.17
Ma5.28
I9.2
Ma3.19
Ma3.3
Ma4.5
Si5.5
Si5.4
Si2(2,3,6,8,10,13,26,29,30)
Si4(4,7)
Ma4(7,12)
I12.4
I12.5
I18.1
Ma1.2
Ma3.7
Ma5.1
Si4.5
Si4.2
Si4.10
Cr1.3
I10(4,12)Ma1(8)
I10(2,5,15)
I10.1
Si5(1,3)
Ma6.7
Si5.2
Ma5(22,24)
Si5.6
Si4.3
Si5.11
I9(4,5)I10(13)I17(3)Ma3(16)Ma6(8,9,11)
I9.1
Ma3.5
Ma5.19
Ma5.23
Ma5.26
Ma6.6
I17.4
Si4.6
T2.1
T2.5
T2.3
T2.4
A19.1
A20.2
Cr1.6
Cr1.10
A20(1)Cr1(4)
A20.3
A21.1
A20(6,7)
A22.1
Co10.2
Co10.20
Co10.21
Co10.27
Co10.11
Co10.6
Co10.16
Co10(1,8)
Co2.6
Co2.16
Co2.20
Co2.24
Co2.26
Co2.31
Co4.1
Co4.9
Co4.11
Co4.12
Co4.13
Co4(5,7)
Co4(8,20)
Co9.1
Co9.3
Co9.2
I11(1-4,8,11,12)
I13.1
I13.4
I13.5
I14.2
Si6(1-6,8,15,18)
I11.15
I14.5
Si3(5,6,9)
Si3.13
Si3(19,22)
Si3(8,16,18)
Si4.1
Si4.8
Si4.9
T1.1
T1.2
T1.3
T1.4
T4.1
T6.6
T6.13
T6.2
T6.5
T6.12
T6.7
T6.3
T6.4
pp ≥ 99
pp ≥ 95
(a)
G
F
E
C.a.max
0.04
Joins Part 2
Shell scale
2cm
0.04

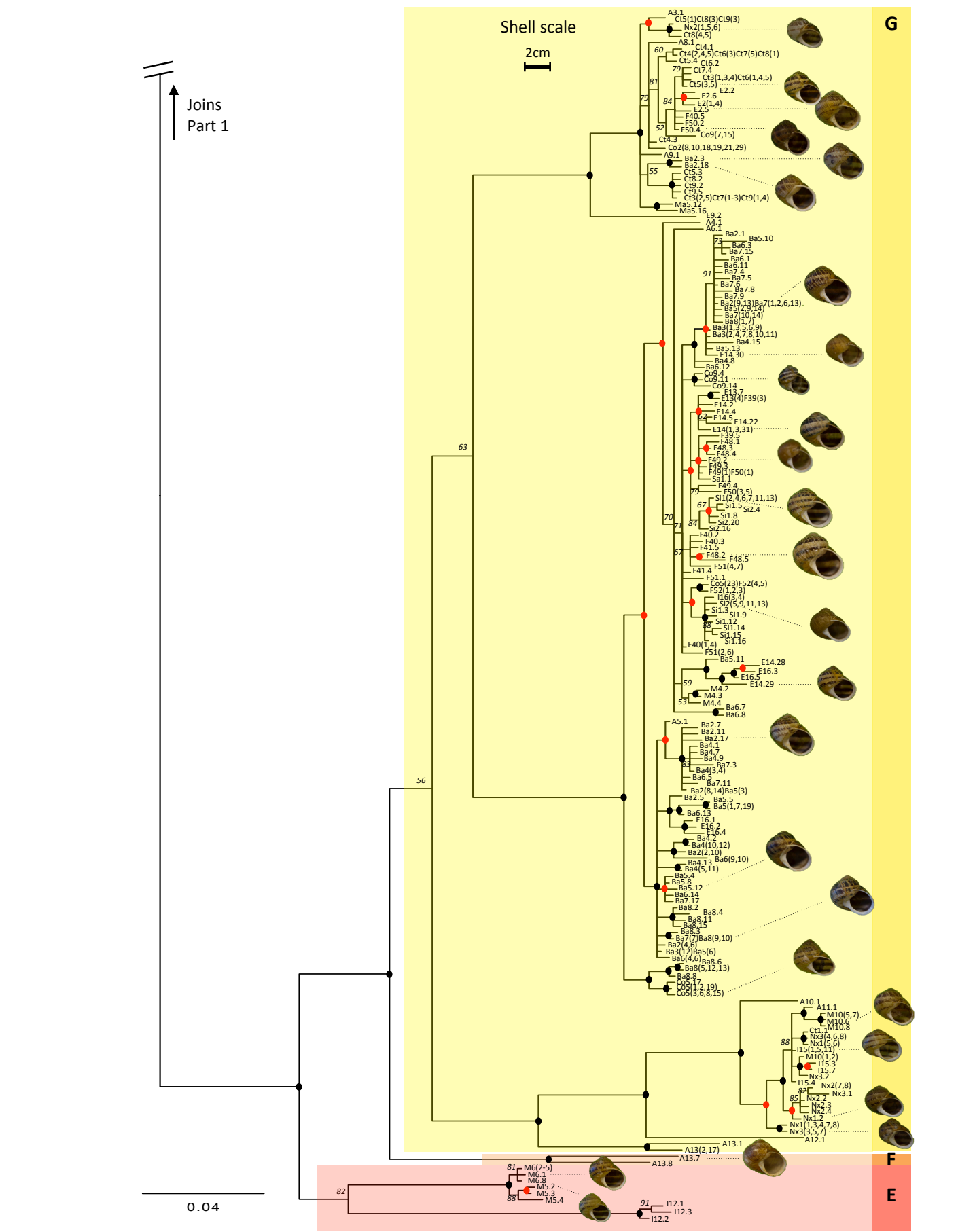
Joins
Part 1
Shell scale
2cm
G
F
E
0.04

Fig. 4

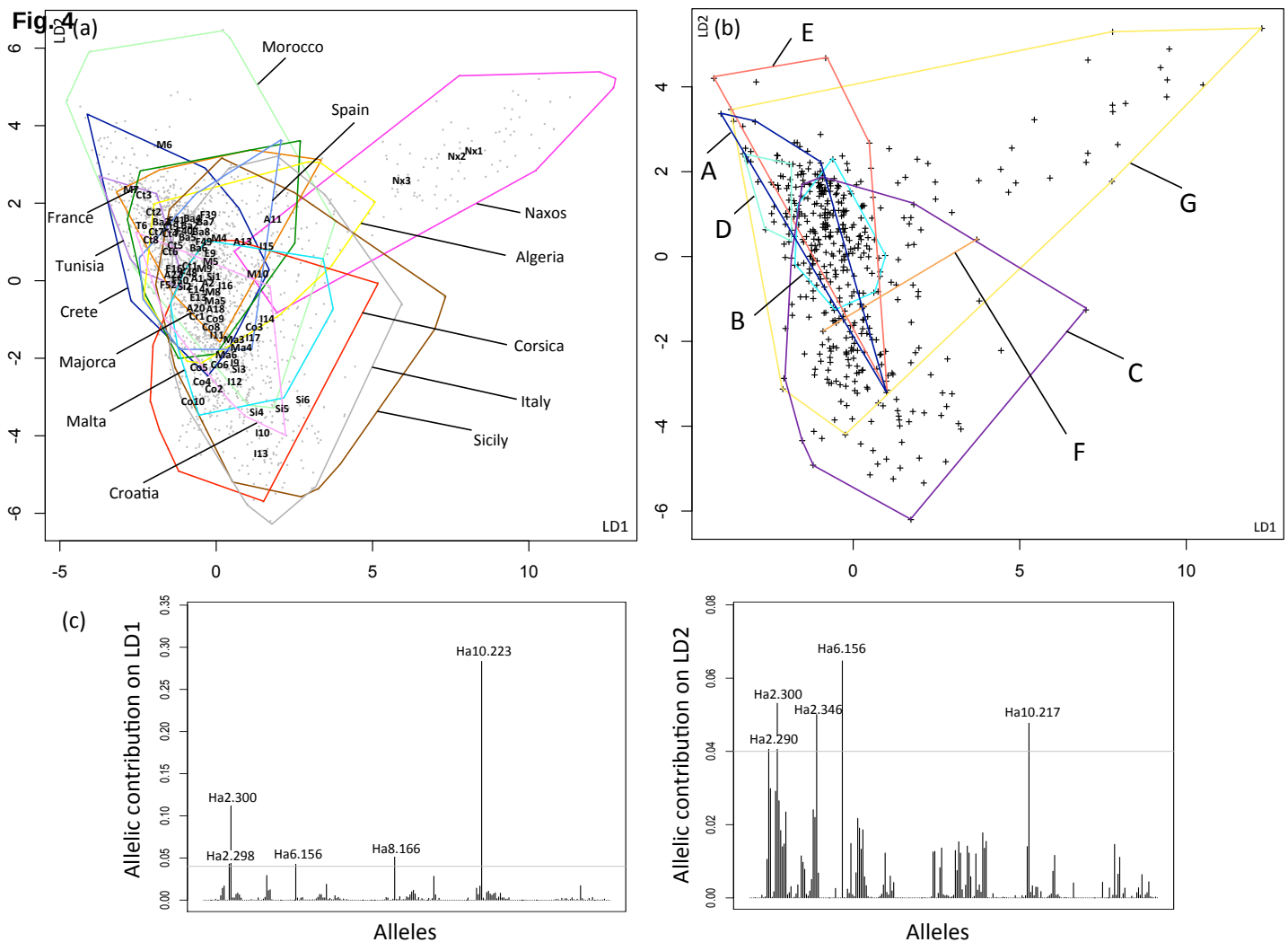
(a)
LD2
LD1
Morocco
Spain
Naxos
Algeria
Corsica
Italy
Sicily
Croatia
Malta
Majorca
Crete
Tunisia
France
(b)
LD2
LD1
A
B
C
D
E
F
G
(c)
Allelic contribution on LD1
Alleles
Ha10.223
Ha2.300
Ha2.298
Ha6.156
Ha8.166
Allelic contribution on LD2
Alleles
Ha6.156
Ha2.300
Ha2.346
Ha2.290
Ha10.217

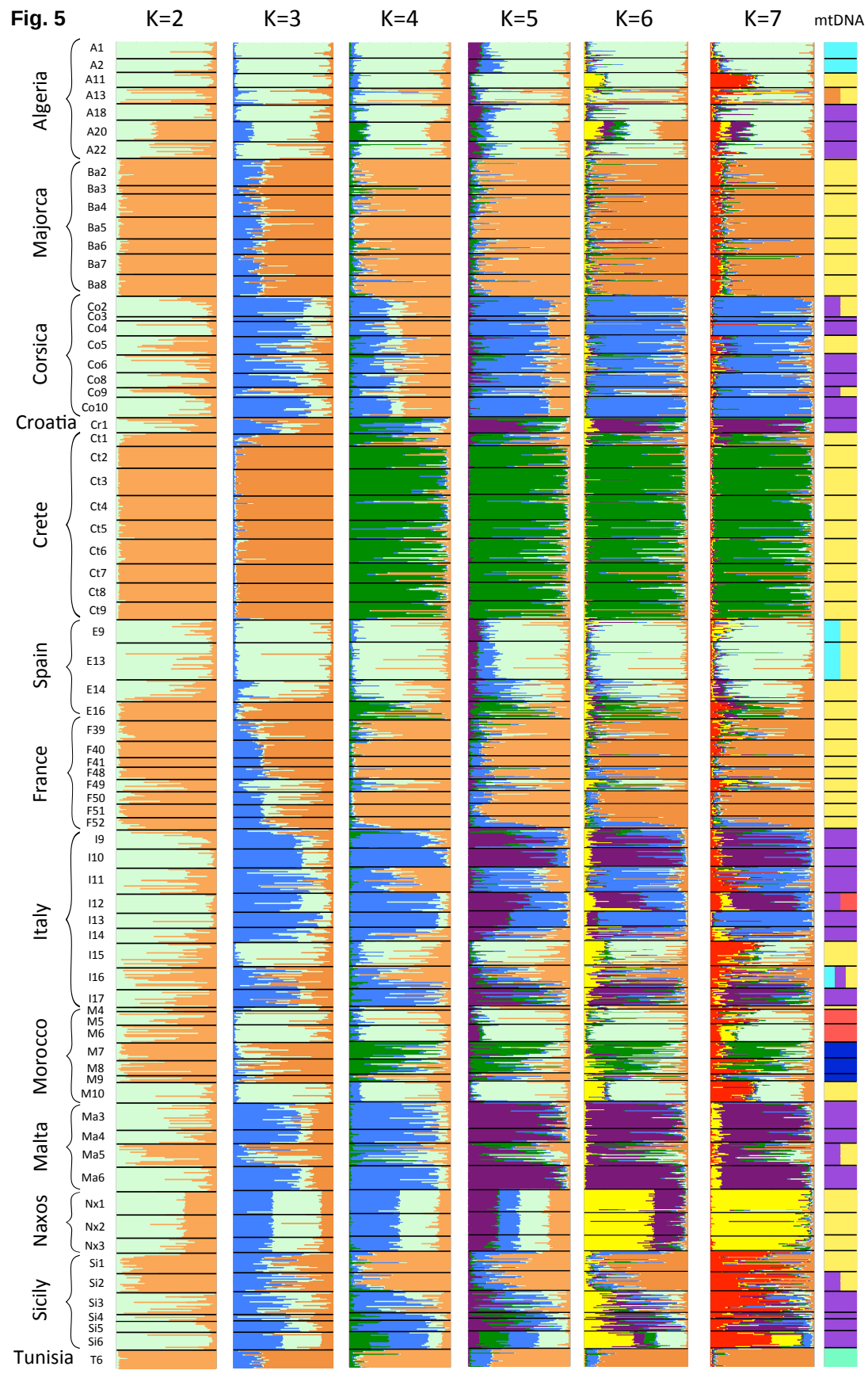
Fig. 5
K=2
K=3
K=4
K=5
K=6
K=7
mtDNA
Algeria
A1
A2
A11
A13
A18
A20
A22
Majorca
Ba2
Ba3
Ba4
Ba5
Ba6
Ba7
Ba8
Corsica
Co2
Co3
Co4
Co5
Co6
Co8
Co9
Co10
Croatia
Cr1
Crete
Ct1
Ct2
Ct3
Ct4
Ct5
Ct6
Ct7
Ct8
Ct9
Spain
E9
E13
E14
E16
France
F39
F40
F41
F48
F49
F50
F51
F52
Italy
I9
I10
I11
I12
I13
I14
I15
I16
I17
Morocco
M4
M5
M6
M7
M8
M9
M10
Malta
Ma3
Ma4
Ma5
Ma6
Naxos
Nx1
Nx2
Nx3
Sicily
Si1
Si2
Si3
Si4
Si5
Si6
Tunisia
T6

Fig. 6

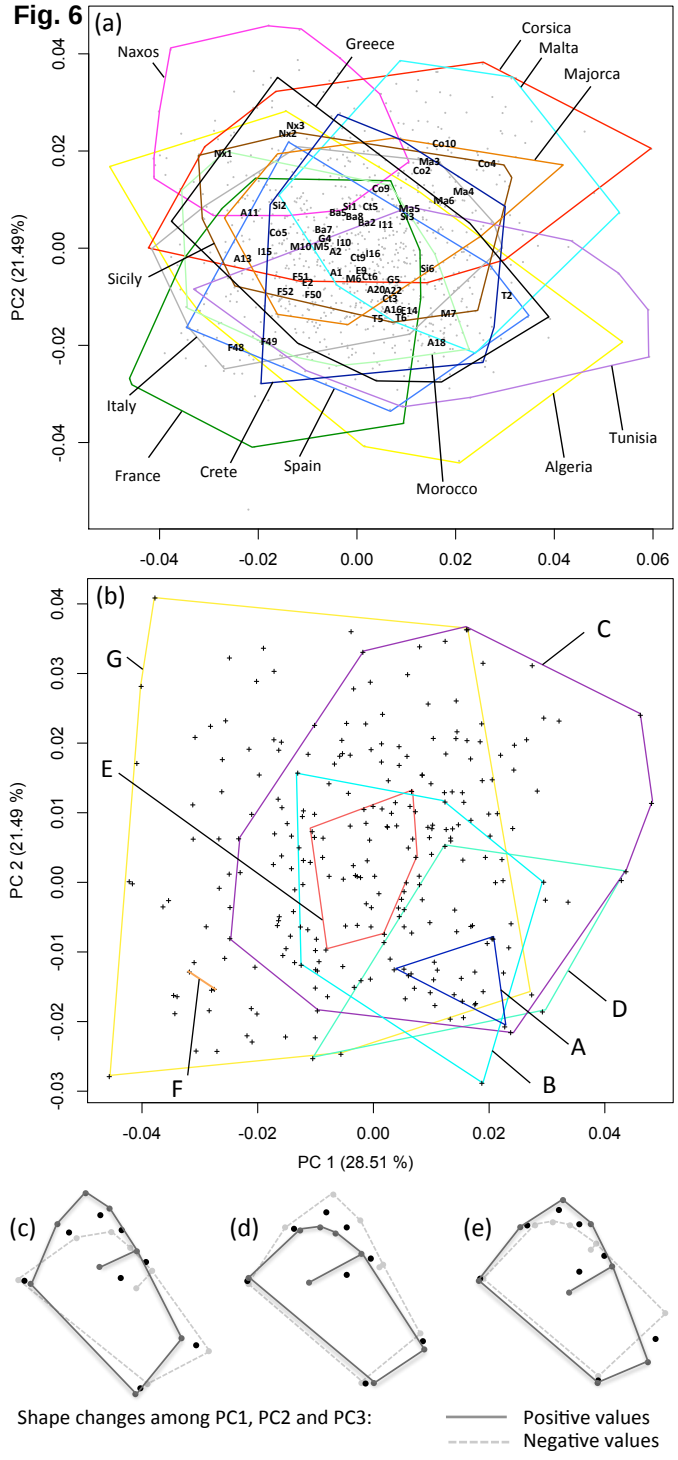
(a)
Naxos
Greece
Corsica
Malta
Majorca
Sicily
Italy
France
Crete
Spain
Morocco
Algeria
Tunisia
PC2 (21.49%)
(b)
G
C
E
D
A
B
F
PC 2 (21.49 %)
PC 1 (28.51 %)
(c)
(d)
(e)
Shape changes among PC1, PC2 and PC3:
Positive values
Negative values

Fig. 7

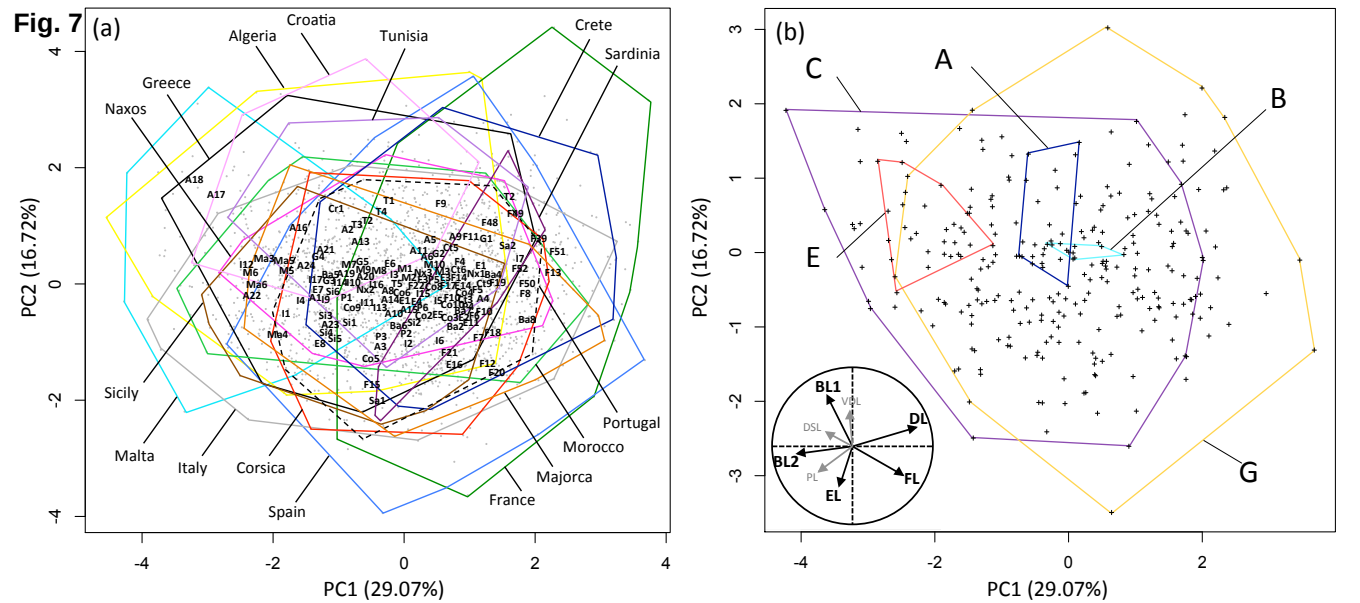
(a)
Croatia
Algeria
Tunisia
Crete
Sardinia
Greece
Naxos
Sicily
Malta
Italy
Corsica
Spain
France
Majorca
Morocco
Portugal
PC1 (29.07%)
PC2 (16.72%)
(b)
A
B
C
E
G
BL1
VSL
DL
DSL
BL2
PL
EL
FL
PC1 (29.07%)
PC2 (16.72%)

Fig. 8

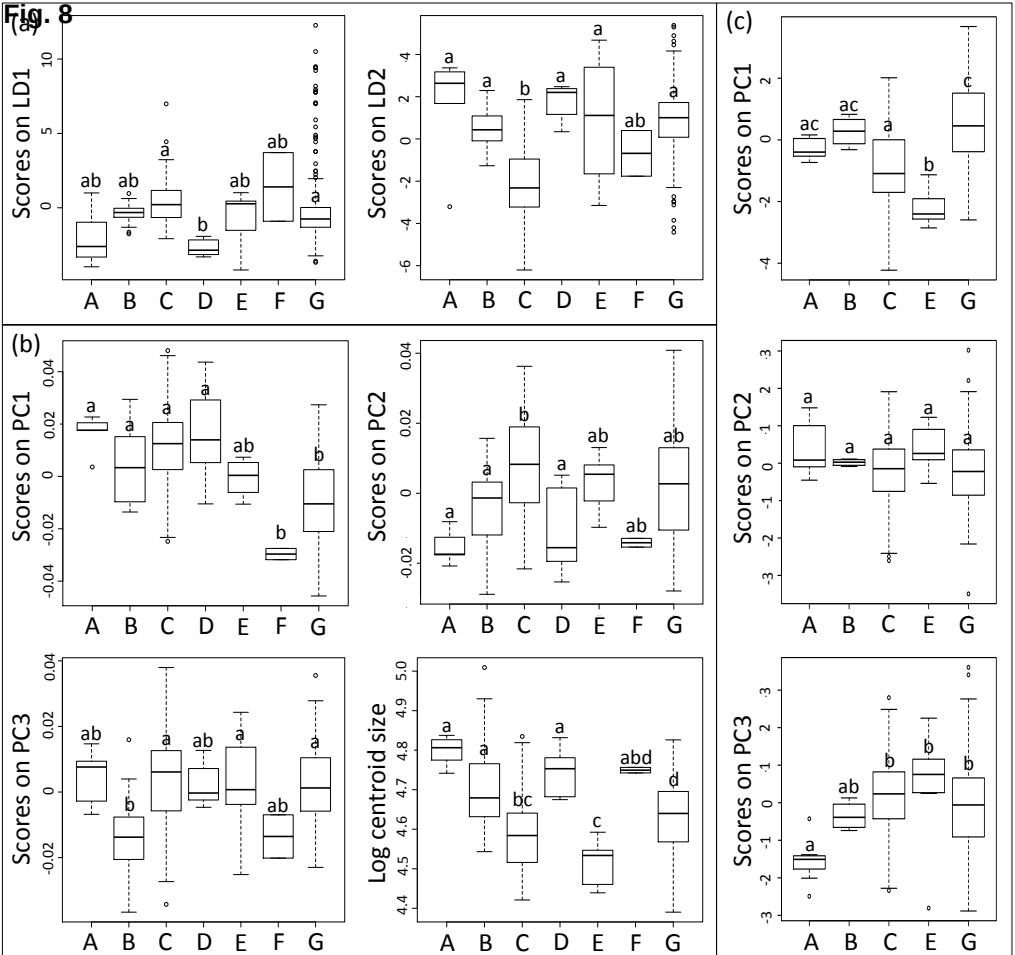
(a)
Scores on LD1
Scores on LD2
(b)
Scores on PC1
Scores on PC2
Scores on PC3
Log centroid size
(c)
Scores on PC1
Scores on PC2
Scores on PC3
A B C D E F G

Table 1. Genetic diversity estimates for 16S and cyt b genes in molecular (mtDNA) and geographical subdivisions.

	Ns		Nh		H ± sd		θπ ± sd	
	16S	cyt b	16S	cyt b	16S	cyt b	16S	cyt b
Molecular subdivisions								
All	499		150	252	0.987 ± 0.002	0.994 ± 0.001	0.047 ± 0.001	0.101 ± 0.001
A	7		6	6	0.952 ± 0.096	0.952 ± 0.096	0.008 ± 0.002	0.008 ± 0.002
B	24		10	11	0.833 ± 0.061	0.884 ± 0.040	0.023 ± 0.003	0.046 ± 0.006
C	155		51	80	0.961 ± 0.005	0.979 ± 0.004	0.020 ± 0.001	0.047 ± 0.002
D	13		11	10	0.974 ± 0.039	0.949 ± 0.051	0.022 ± 0.002	0.040 ± 0.005
E	12		3	8	0.530 ± 0.136	0.848 ± 0.104	0.035 ± 0.011	0.051 ± 0.015
F	2		2	2	1.000 ± 0.500	1.000 ± 0.500	0.036 ± 0.018	0.068 ± 0.034
G	286		82	137	0.952 ± 0.005	0.988 ±0.002	0.036 ± 0.002	0.066 ± 0.003
Geographical subdivisions								
All	601	592	177	291	0.979 ± 0.002	0.994 ± 0.001	0.045 ± 0.001	0.102 ± 0.001
Algeria	36	46	28	39	0.983 ± 0.011	0.992 ± 0.006	0.051 ± 0.004	0.112 ± 0.004
Corsica	67	55	21	40	0.921 ± 0.016	0.977 ± 0.011	0.036 ± 0.003	0.085 ± 0.005
Crete	45	40	10	13	0.819 ± 0.027	0.881 ± 0.026	0.009 ± 0.003	0.021 ± 0.007
Croatia	7	6	4	4	0.714 ± 0.006	0.867 ± 0.129	0.015 ± 0.006	0.025 ± 0.015
France	49	41	26	22	0.900 ± 0.037	0.950 ± 0.018	0.016 ± 0.004	0.019 ± 0.006
Greece	2	0	1	0	-	-	-	-
Italy	52	48	25	21	0.950 ± 0.014	0.946 ± 0.014	0.041 ± 0.005	0.087 ± 0.007
Majorca	101	98	28	50	0.876 ± 0.021	0.954 ± 0.014	0.009 ± 0.001	0.017 ± 0.002
Malta	32	33	10	19	0.869 ± 0.035	0.945 ± 0.023	0.022 ± 0.005	0.042 ± 0.008
Morocco	29	31	12	18	0.837 ± 0.049	0.953 ± 0.021	0.058 ± 0.003	0.094 ± 0.005
Naxos	24	24	7	7	0.848 ± 0.001	0.815 ± 0.046	0.020 ± 0.007	0.032 ± 0.011
Sardinia	4	7	4	7	1.000 ± 0.177	1.000 ± 0.076	0.031 ± 0.013	0.041 ± 0.015
Sicily	78	97	17	26	0.882 ± 0.016	0.929 ± 0.011	0.030 ± 0.001	0.079 ± 0.087
Spain	48	46	17	28	0.900 ± 0.026	0.952 ± 0.018	0.045 ± 0.001	0.097 ± 0.003
Tunisia	21	20	16	15	0.971 ± 0.023	0.963 ± 0.028	0.033 ± 0.006	0.068 ± 0.006

Ns, number of sequences; Nh, number of haplotypes (excluding gaps and missing data); H, haplotype diversity; θπ, nucleotide diversity; sd, standard deviation.

Table 2. Results of one-way ANOVAs performed with individuals' scores on each multivariate variable according to mtDNA clades and Mantel tests performed between pairwise distances based on microsatellite genotypes (DSA) or morphometric traits (individual scores) and phylogenetic branch lengths.

Variables	Variables information	N	ANOVA		Mantel	
			mtDNA clades		Phylogenetic distances	
			F	p*	r	p*
Microsatellite		460				
LD1	Ha10.223, Ha2.298, Ha2.300, Ha6.156, Ha8.166		4.295	<0.001		
LD2	Ha2.290, Ha2.300, Ha2.346, Ha6.156, Ha10.217		60.97	<0.001		
DSA	Shared allele distance				0.15	<0.001
Shell shape		264				
PC1	Elongated vs. globular		19.55	<0.001	0.19	<0.001
PC2	Large vs. small aperture		4.99	<0.001	0.04	0.002
PC3	Rounded vs. oval aperture		6.06	<0.001	0.02	0.080
Shell size	Log centroid size	264	12.77	<0.001	0.04	0.004
Genitalia variables		281				
PC1	DL and FL vs. BL2		24.83	<0.001	0.12	<0.001
PC2	BL1 vs. EL		1.80	0.128	0.00	0.48
PC3	VDL and DSL vs. BL1		5.22	<0.001	0.00	0.40

N, sample size; r, correlation coefficient; *, standard Bonferroni correction.

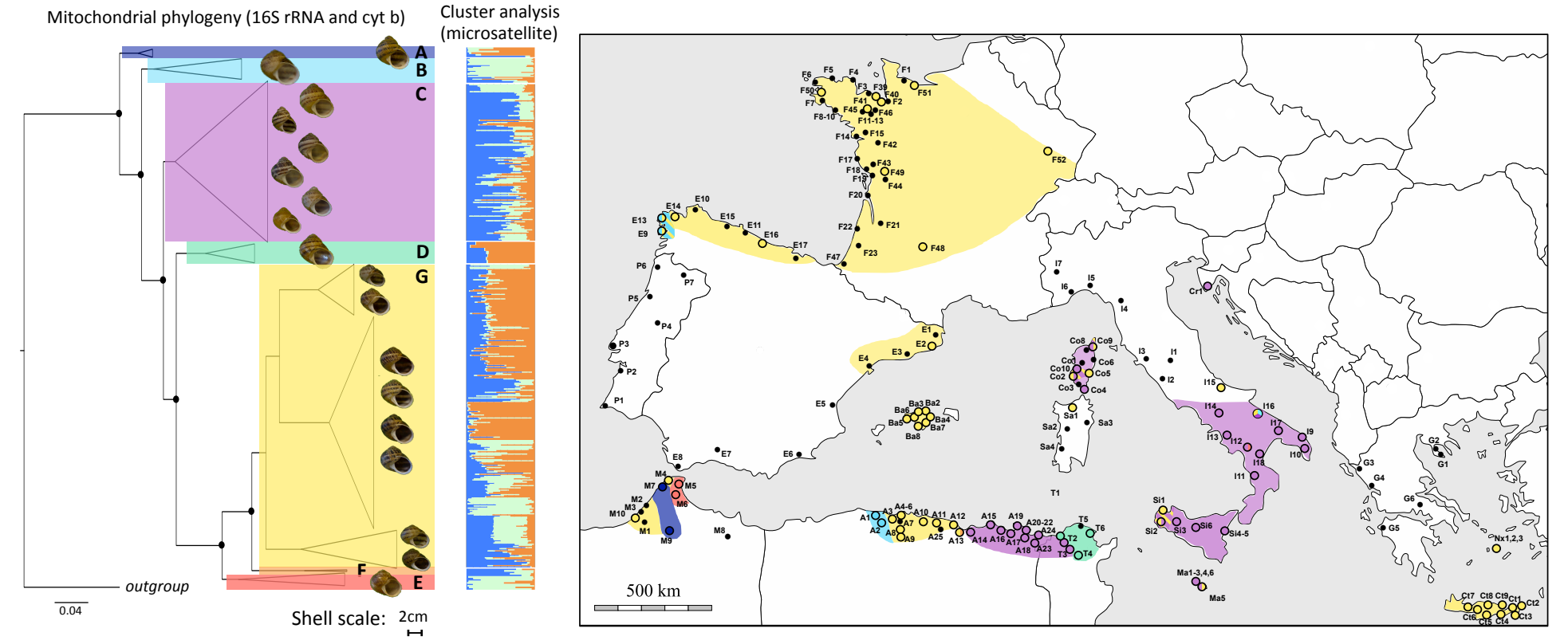
Mitochondrial phylogeny (16S rRNA and cyt b)
Cluster analysis (microsatellite)
A
B
C
D
G
F
E
outgroup
0.04
Shell scale: 2cm
500 km

Highlights

- Well-sampled Mediterranean basin recovers a novel phylogeny of *Cornu aspersum aspersum*.
- The mitochondrial phylogeny was compared with morphological traits and microsatellite genotypes.
- Clades diversification supports the hypothesis of multiple refugial areas in North Africa.
- We propose a new biogeographical scenario with two contrasting patterns of dispersal in the Mediterranean.